Optimal Designs of the Synthetic t Chart with Estimated Process Mean

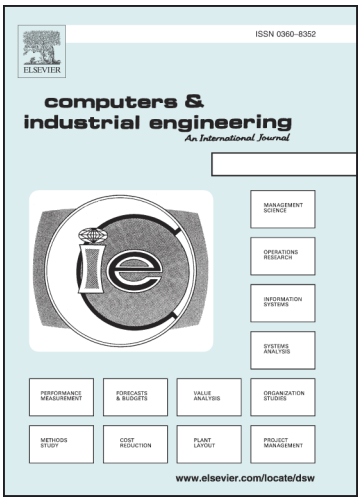

Optimal Designs of the Synthetic *t* Chart with Estimated Process Mean

W.L. Teoh, S.K. Chuah, Michael B.C. Khoo, Philippe Castagliola, W.C. Yeong

PII: S0360-8352(17)30380-7
DOI: http://dx.doi.org/10.1016/j.cie.2017.08.021
Reference: CAIE 4868

To appear in: *Computers & Industrial Engineering*

Received Date: 29 January 2016
Revised Date: 8 June 2017
Accepted Date: 16 August 2017

Please cite this article as: Teoh, W.L., Chuah, S.K., Khoo, M.B.C., Castagliola, P., Yeong, W.C., Optimal Designs of the Synthetic *t* Chart with Estimated Process Mean, *Computers & Industrial Engineering* (2017), doi: http://dx.doi.org/10.1016/j.cie.2017.08.021

Optimal Designs of the Synthetic *t* Chart with Estimated Process Mean

W.L. Teoh (Corresponding author)
School of Mathematical and Computer Sciences
Heriot-Watt University Malaysia,
62200 Putrajaya, Malaysia
weilin.teoh@gmail.com
Tel: +603-88943888; Fax: +603-88943999

S.K. Chuah
Department of Physical and Mathematical Sciences,
Faculty of Science,
Universiti Tunku Abdul Rahman, 31900 Kampar, Perak, Malaysia
skeleog@gmail.com

Michael B.C. Khoo
School of Mathematical Sciences
Universiti Sains Malaysia, 11800 Penang, Malaysia
mkbc@usm.my

Philippe Castagliola
Department of Quality and Logistics
LUNAM Université, Université de Nantes & IRCCyN UMR CNRS 6597, Carquefou, France
philippe.castagliola@univ-nantes.fr

W.C. Yeong
Department of Operations and Management Information Systems,
Faculty of Business and Accountancy,
Universiti Malaya, 50603 Kuala Lumpur, Malaysia
yeongwc@um.edu.my

Optimal Designs of the Synthetic *t* Chart with Estimated Process Mean

Abstract

The synthetic *t* chart, which integrates a *t* chart and a conforming run length chart, is robust against changes in the process standard deviation. Traditionally, the synthetic *t* chart is studied by assuming that the in-control process mean is known. Practically, this is not always the case. The process mean is rarely known and it has to be estimated from a Phase-I dataset. Therefore, this paper presents the Markov chain approach for studying the run-length properties of the synthetic *t* chart with estimated process mean for both zero- and steady-state cases. The impact of the mean estimation on the synthetic *t* chart is evaluated and compared with its known-process-mean counterpart and the synthetic $\bar{X}$ chart. For optimum implementation, this paper develops two optimal design strategies for the synthetic *t* chart with estimated process mean, by minimizing (i) the average run length (ARL) and (ii) the expected ARL, for deterministic and unknown shift sizes, respectively. By taking the number of Phase-I samples and sample sizes adopted in practice into consideration, tables listing the new optimal charting parameters of the proposed chart are provided in this paper. Comparative studies show that there are some potential benefits, especially the desirable robustness property, of the synthetic *t* chart with estimated process mean over the synthetic $\bar{X}$, Shewhart $\bar{X}$ and *t* charts with estimated process parameters or mean. The application of the synthetic *t* chart with estimated process mean is illustrated with real industrial data gathered from a silicon epitaxy process.

Keywords: Average run length; Optimal design; Parameter estimation; Robustness; Synthetic *t* chart; Unknown shift size.

1. Introduction

Control chart is one of the prevalent tools in Statistical Process Control (SPC). It is widely used to monitor the process mean and / or variation in order to improve the quality and performance of a process. Owing to its operational simplicity, the Shewhart $\bar{X}$ chart is the most popular control chart among all types of control charts in determining whether a process is in a state of statistical control. To operate this chart effectively, it is often assumed that the process standard deviation used to establish the control chart's limits can be estimated without any error. This assumption may fail, either because there are insufficient

in-control data or the process standard deviation has changed. Consequently, a deterioration of the $\bar{X}$ chart's performance occurs (Zhang et al., 2009). A signal given by the $\bar{X}$ chart under such circumstances is questionable as this signal could be genuinely due to an out-of-control status or it could be due to a false alarm. This shows that the $\bar{X}$ -type charts are not robust and quite confusing when the process standard deviation is unstable. Therefore, Zhang et al. (2009) introduced the *t* and the exponentially weighted moving average (EWMA) *t* charts, which do not require the estimation of the process standard deviation during Phase-I analysis. Also, they demonstrated that both the *t* and EWMA *t* charts have more desirable robustness against changes in the process standard deviation compared to the Shewhart $\bar{X}$ and EWMA $\bar{X}$ charts. The synthetic *t* and the synthetic EWMA *t* charts proposed by Calzada and Scariano (2013) not only enhance the performance of the *t* and EWMA *t* charts, respectively, but they also maintain the desirable robustness property of these *t*-type charts. Moreover, Castagliola et al. (2013b) presented the variable sample size (VSS) *t* chart for monitoring short-run processes. They concluded that the VSS *t* chart is statistically superior to the *t* chart for moderate to large shifts. In an effort to improve the statistical efficiency over the EWMA *t* chart, Kazemzadeh et al. (2013) suggested the variable sampling interval (VSI) EWMA *t* chart. The run sum *t* chart proposed by Sitt et al. (2014) is more robust compared to the run sum $\bar{X}$ chart for small mean shifts and it surpasses the EWMA *t* chart for moderate to large mean shifts.

In the existing literature, most of the $\bar{X}$ -type and *t*-type control charts are constructed and developed under the assumption that the in-control process parameters (mean and / or standard deviation) are perfectly known. However, the process parameters are rarely known in practice. They are estimated by using a finite in-control Phase-I historical dataset. When the process parameters are estimated, the statistical performance of the control charts is significantly different from that of the case where the process parameters are known. This is because of the variability of the parameter estimators in the Phase-I process. Jensen et al. (2006) and Psarakis et al. (2014) extensively discussed the developments on the impacts of parameter estimation on numerous control charts. Much efforts have been devoted to the $\bar{X}$ -type control charts, for example, see the discussions by Zhang et al. (2011), Castagliola et al. (2012) and Teoh et al. (2014); while Castagliola and Maravelakis (2011), Faraz et al. (2015) and Guo et al. (2015) contributed to the dispersion-type control charts with unknown variance. While there are various *t*-type control charts developed in the existing literature, to date, all the existing *t*-type control charts are designed based on a known process mean,

except the *t* chart with estimated process mean proposed by Castagliola et al. (2013a). Undoubtedly, it is high time that more researches need to be conducted for designing the *t*-type control charts, accounting for the process mean estimation.

The synthetic $\bar{X}$ chart, comprising the Shewhart $\bar{X}$ and the conforming run length (*CRL*) charts, was introduced by Wu and Spedding (2000). They showed that the synthetic $\bar{X}$ chart outperforms the Shewhart $\bar{X}$, joint $\bar{X}$-EWMA and EWMA charts for detecting a wide range of process mean shifts. Davis and Woodall (2002) mentioned that the synthetic chart can be considered as a runs-rule-type chart with a head-start feature. They also formulated a Markov chain model to evaluate the zero- and steady-state average run lengths (*ARLs*). Aparisi and de Luna (2009) optimized the synthetic $\bar{X}$ chart with the aim of detecting important shifts in the out-of-control region, without detecting shifts in an admissible shift region. It was shown by Wu et al. (2010) that a combined synthetic and *X* chart improves the statistical performance of the individual synthetic chart and the individual *X* chart by 20% and 47%, respectively. Recently, a combined side-sensitive synthetic chart and VSS $\bar{X}$ chart was proposed by Costa and Machado (2016). They claimed that the synthetic chart's performance is always enhanced by the side-sensitive feature. Due to the growing interests in the synthetic-type control charts, the synthetic feature has also been extended to the synthetic dispersion chart (Huang and Chen, 2005), synthetic double sampling *np* chart for attribute (Chong et al., 2014) and synthetic chart for simultaneously monitoring process mean and variance (Costa et al., 2009).

The synthetic-type charts are commonly applied in industrial processes. Wu et al. (2001) implemented the synthetic chart for monitoring an increase in the fraction nonconforming of a process in an electronics company. The synthetic-type $\bar{X}$ charts are successfully applied to monitor the tensile strength of fibers used in manufacturing cloths (Costa and Machado, 2016), the flow width of the resist in a hard-bake process (Haq et al., 2016a), and the dimension of the die on each wafer in a photolithography process (Wu et al., 2010). It is common in the manufacturing sector that careless or unskilled operators, inferior raw materials, and loosening of machine settings will lead to a change in the process dispersion. Therefore, the synthetic-type charts for monitoring process dispersion are used to monitor the quantity of content in a yogurt cup filling process (Guo et al., 2015), soda can filling process (Haq et al., 2016b), and juice filling process (Huang and Chen, 2005).

To avoid unwanted deterioration of control charts' performance from estimation errors, in this paper, we propose the synthetic *t* chart with estimated process mean. By using the

Markov chain approach, we derive the mathematical expressions for the zero- and steady-state *ARLs* and standard deviation of the run lengths (*SDRLs*) of the synthetic *t* chart when the process mean is estimated. For optimum implementation of the synthetic *t* chart with estimated process mean in manufacturing and service sectors, this paper develops two optimal design strategies for the proposed chart by minimizing (i) the out-of-control *ARL* (ARL_1) and (ii) the out-of-control expected *ARL* ($EARL_1$), for known and unknown shift sizes, respectively. The inclusion of the second optimization criterion comes from the fact that, in practice, it is too restrictive to assume that the shift size is known a priori. A quality practitioner usually does not know the actual shift size in advance. This is either because the shift size may change over time or the historical data are insufficient or absent. Therefore, the expected *ARL* (*EARL*) is evaluated in order to obtain an overall good performance over a shift domain.

The remainder of the paper is structured as follows: The synthetic *t* chart is described in Section 2; while Section 3 details the statistical properties of the synthetic *t* chart with known and estimated process mean. In Section 4, effect of the process mean estimation on the synthetic *t* chart is compared with its known-process-mean counterpart and the synthetic $\bar{X}$ chart with known and estimated process parameters. Section 5 describes the two optimal design strategies of the synthetic *t* chart with estimated process mean, for both the known- and unknown-shift-size conditions. In Section 6, the construction of the synthetic *t* chart with estimated process mean is illustrated with a real industrial dataset from a silicon epitaxy process. Section 7 studies the robustness of the synthetic *t* chart with estimated process mean. Also, the run-length performance of the *t*, $\bar{X}$, synthetic *t* and synthetic $\bar{X}$ charts with estimated process mean or parameters are compared in this section. Finally, some remarks are concluded in Section 8.

2. The synthetic *t* chart

The synthetic *t* chart integrates a *t* chart and a *CRL* chart. It consists of a *t/S* sub-chart and a *CRL/S* sub-chart. The *CRL* denotes the number of inspected samples between two successive non-conforming samples, inclusive of the ending non-conforming sample. Suppose that a process starts at $t = 0$, then Fig. 1 provides an example explaining how the *CRL* values are obtained. From Fig. 1, it is shown that $CRL_1 = 4$, $CRL_2 = 2$ and $CRL_3 = 3$.

[Insert Figs. 1 and 2 here.]

With the aid of the flow diagram shown in Fig. 2, the steps to construct and implement the synthetic *t* chart are demonstrated as follows:

Step 1. Determine the lower limit, $L \in \{1, 2, \ldots\}$ of the *CRL/S* sub-chart. Then determine the upper (UCL_t) and lower (LCL_t) control limits of the *t/S* sub-chart as follows:

$$UCL_t = K = -LCL_t . \quad (1)$$

Note that when the process is in-control (i.e., in-control mean, $\mu_0 = 0$), the plotting statistic T_i (see Eq. (2)), for $i = 1, 2, \ldots$, of the Synthetic *t* chart has a central Student's *t* distribution with $(n-1)$ degrees of freedom.

Step 2. Take a random sample of size *n* at each inspection point *i*. Then compute the sample mean ($\bar{Y}_i$), standard deviation (S_i) and the monitored statistic is

$$T_i = \frac{(\bar{Y}_i - \mu_0)\sqrt{n}}{S_i}, \text{ for } i = 1, 2, \ldots \quad (2)$$

Step 3. Classify the sample as conforming if $LCL_t < T_i < UCL_t$. Then the control flow returns to Step 2; otherwise, the sample is non-conforming and the control flow proceeds to Step 4.

Step 4. Count the number of T_i samples between the current (included) and the previous (excluded) non-conforming samples as the *CRL* value.

Step 5. Declare the process as in-control if $CRL \geq L$ and the control flow returns to Step 2; otherwise, proceed to Step 6.

Step 6. Signal an out-of-control status.

Step 7. Find and remove the assignable cause(s). Then, return to Step 2.

3. The run-length properties of the synthetic *t* chart

3.1. The synthetic t chart with known process mean

Calzada and Scariano (2013) proposed a direct method to evaluate the run-length properties of the synthetic *t* chart. However, only the zero-state *ARL* and *SDRL* can be computed from this direct method. On the other hand, although the Markov chain approach presented by Davis and Woodall (2002) is more complex, it allows us to evaluate the *ARL*, *SDRL*, probability mass function (pmf) and cumulative distribution function (cdf) of the run length of the synthetic *t* chart under both the zero- and steady-state cases. Therefore, the Markov chain approach is adopted in this paper to evaluate the performance of the synthetic *t*

chart. The (L+2, L+2) transition probability matrix **P** of the synthetic t chart has the following structure:

$$\mathbf{P} = \begin{pmatrix} \mathbf{Q} & \mathbf{r} \\ \mathbf{0}^T & 1 \end{pmatrix} = \left(\begin{array}{cccccc|c} 1-p & p & 0 & \cdots & \cdots & 0 & 0 \\ 0 & 0 & 1-p & \ddots & & 0 & p \\ \vdots & & \ddots & \ddots & \ddots & \vdots & \vdots \\ \vdots & & & \ddots & 1-p & 0 & \vdots \\ 0 & \cdots & \cdots & \cdots & 0 & 1-p & p \\ 1-p & 0 & \cdots & \cdots & \cdots & 0 & p \\ \hline 0 & \cdots & \cdots & \cdots & \cdots & 0 & 1 \end{array}\right), \tag{3}$$

where **Q** is the (L+1, L+1) matrix of transient probabilities, $\mathbf{0} = (0, 0, \ldots, 0)^T$ and **r** is the (L+1, 1) vector satisfying $\mathbf{r} = \mathbf{1} - \mathbf{Q1}$, for $\mathbf{1} = (1, 1, \ldots, 1)^T$. The probability p is equal to

$$\begin{aligned} p &= \Pr\left(T_i \notin \left[LCL_t, UCL_t\right]\right) \\ &= 1 - F_t\left(UCL_t \middle| n-1, \frac{\delta\sqrt{n}}{\tau}\right) + F_t\left(LCL_t \middle| n-1, \frac{\delta\sqrt{n}}{\tau}\right), \end{aligned} \tag{4}$$

where $F_t\left(\cdot \middle| n-1, \lambda\right)$ is the cdf of a non-central Student's t-distribution with non-centrality parameter λ and $n-1$ degrees of freedom. In Eq. (4), $\delta = \left|\mu_1 - \mu_0\right| / \sigma_0$ is the magnitude of a standardized mean shift with the out-of-control mean μ_1; while $\tau > 0$ is the magnitude of the process variance shift. If δ = 0 and τ = 1, the process is in-control; otherwise, it is out-of-control.

Let H be the number of steps until the process reaches the absorbing state. Neuts (1981) and Latouche and Ramaswami (1999) explained that H is a *Discrete PHase-type* (DPH) random variable of parameters (**Q**, **q**), where **q** is the initial probability vector. For the zero-state case, the initial probability vector is $\mathbf{q} = \mathbf{q}_{ini} = (0, 1, 0, \ldots, 0)^T$; while that for the steady-state case, it is $\mathbf{q} = \mathbf{q}_{ss}$ (see Eq. (9)). The zero-state pmf, $f_H\left(h\right)$ and cdf, $F_H\left(h\right)$ of H are defined as

$$f_H\left(h\right) = \mathbf{q}_{ini}^T \mathbf{Q}^{h-1} \mathbf{r} \tag{5}$$

and

$$F_H\left(h\right) = 1 - \mathbf{q}_{ini}^T \mathbf{Q}^h \mathbf{1}, \tag{6}$$

respectively, for $h \in \{1, 2, 3, \ldots\}$. Then the zero-state $ARL = E(H)$ and $SDRL = \sigma(H)$ of the synthetic t chart are

$$ARL = \mathbf{q}_{ini}^T \left(\mathbf{I} - \mathbf{Q}\right)^{-1} \mathbf{1} \tag{7}$$

and

$$SDRL = \sqrt{2\mathbf{q}_{ini}^{T}\left(\mathbf{I}-\mathbf{Q}\right)^{-2}\mathbf{Q1} - ARL^{2} + ARL}\,, \tag{8}$$

respectively, where **I** is the $(L+1, L+1)$ identity matrix. Note that the zero-state *ARL* and *SDRL* values computed using the Calzada and Scariano's (2013) direct method are exactly the same as the ones computed using the Markov chain method.

The steady-state pmf, cdf, *ARL* and *SDRL* can easily be computed by replacing the initial probability vector $\mathbf{q}_{ini}$ in Eqs. (5) to (8), respectively, with the cyclical steady-state probability vector $\mathbf{q}_{ss}$. By applying Darroch and Seneta's (1965) method, the cyclical steady-state probability vector $\mathbf{q}_{ss}$ can easily be obtained as

$$\mathbf{q}_{ss} = \frac{\left(\mathbf{I}-\mathbf{Q}^{T}\right)^{-1}\mathbf{q}_{ini}}{\mathbf{1}^{T}\left(\mathbf{I}-\mathbf{Q}^{T}\right)^{-1}\mathbf{q}_{ini}}\,. \tag{9}$$

3.2. The synthetic t chart with estimated process mean

When the in-control process mean μ_0 is unknown, it is estimated from a Phase-I data set of *m* subgroups $\{X_{i,1}, X_{i,2}, \ldots, X_{i,n}\}$, each having *n* observations, for $i = 1, 2, \ldots, m$. It is important to note that, unlike the synthetic $\bar{X}$ chart with estimated process parameters, the synthetic *t* chart with estimated process mean does not involve estimating σ_0 in the computation of the plotting statistic and the construction of the control chart's limits. Let us assume that there is independence within and between subgroups and that $X_{i,j} \sim N(\mu_0, \sigma_0^2)$. A commonly used estimator $\hat{\mu}_0$ of μ_0 is equal to

$$\hat{\mu}_0 = \frac{1}{mn}\sum_{i=1}^{m}\sum_{j=1}^{n} X_{i,j}\,. \tag{10}$$

When the process mean μ_0 is estimated, the control limits UCL_t and LCL_t in Eq. (1) of the synthetic *t/S* sub-chart become

$$\widehat{UCL}_t = K = -\widehat{LCL}_t; \tag{11}$$

while the random variable T_i in Eq. (2) becomes $\hat{T}_i$, where μ_0 is replaced by $\hat{\mu}_0$, i.e.

$$\hat{T}_i = \frac{\left(\bar{Y}_i - \hat{\mu}_0\right)\sqrt{n}}{S_i}, \text{ for } i = 1, 2, \ldots \tag{12}$$

For a fixed $\hat{\mu}_0$ value, the conditional zero-state pmf $f_H(h)$ and cdf $F_H(h)$ of the run length *H* of the synthetic *t* chart are shown in Eqs. (5) and (6), respectively. When the process

mean μ_0 is estimated, the unconditional zero-state pmf $f_H(h)$ and cdf $F_H(h)$ of the run length *H* of the synthetic *t* chart are equal to

$$f_H(h) = \int_{-\infty}^{+\infty} \left(\mathbf{q}_{ini}^T \hat{\mathbf{Q}}^{h-1} \hat{\mathbf{r}} \right) f_U(u|m)\, du \tag{13}$$

and

$$F_H(h) = 1 - \int_{-\infty}^{+\infty} \left(\mathbf{q}_{ini}^T \hat{\mathbf{Q}}^{h} \mathbf{1} \right) f_U(u|m)\, du\,, \tag{14}$$

respectively, for $h \in \{1, 2, 3, \ldots\}$. The $\hat{\mathbf{Q}}$ and $\hat{\mathbf{r}}$ in Eqs. (13) and (14) are matrix **Q** and vector **r**, respectively, where the probability *p* is replaced by $\hat{p}$, i.e.

$$\hat{p} = 1 - F_t\left(\widehat{UCL}_t \,\middle|\, n-1, \tfrac{\delta\sqrt{n}+U}{\tau} \right) + F_t\left(\widehat{LCL}_t \,\middle|\, n-1, \tfrac{\delta\sqrt{n}+U}{\tau} \right), \tag{15}$$

where $U \sim N(0, 1/m)$ and $f_U(u|m)$ in Eqs. (13) and (14) is the probability density function (pdf) of the random variable *U*. The derivation of $\hat{p}$ is detailed in Appendix A.

Similarly, the conditional zero-state *ARL* and *SDRL* of the synthetic *t* chart are shown in Eqs. (7) and (8), respectively; while the unconditional zero-state *ARL* and *SDRL* of the synthetic *t* chart with estimated process mean are

$$ARL = \int_{-\infty}^{+\infty} \mathbf{q}_{ini}^T \left(\mathbf{I} - \hat{\mathbf{Q}} \right)^{-1} \mathbf{1}\, f_U(u|m)\, du \tag{16}$$

and

$$SDRL = \sqrt{E\left(H^2\right) - ARL^2}\,, \tag{17}$$

respectively, where

$$E(H^2) = \int_{-\infty}^{+\infty} \left[\mathbf{q}_{ini}^T \left(\mathbf{I} - \hat{\mathbf{Q}} \right)^{-1} \mathbf{1} + 2\mathbf{q}_{ini}^T \left(\mathbf{I} - \hat{\mathbf{Q}} \right)^{-2} \hat{\mathbf{Q}} \mathbf{1} \right] f_U(u|m)\, du\,. \tag{18}$$

For the steady-state case, the pmf, cdf, *ARL* and *SDRL* of the synthetic *t* chart with estimated process mean can also be computed using Eqs. (13), (14), (16) and (17), respectively, in which the initial probability vector $\mathbf{q}_{ini}$ is replaced by the cyclical steady-state probability vector $\hat{\mathbf{q}}_{ss}$, i.e.

$$\hat{\mathbf{q}}_{ss} = \frac{\left(\mathbf{I} - \hat{\mathbf{Q}}^T \right)^{-1} \mathbf{q}_{ini}}{\mathbf{1}^T \left(\mathbf{I} - \hat{\mathbf{Q}}^T \right)^{-1} \mathbf{q}_{ini}}\,. \tag{19}$$

4. Comparison of the performances of the synthetic *t* and synthetic $\bar{X}$ charts with estimated and known process mean or parameters

This paper aims at investigating the impact of estimation errors on the synthetic *t* chart's performance and it is not intended to show the advantage of the synthetic *t* chart with estimated process mean over other control charts. Table 1 shows the zero- and steady-state *ARL* and *SDRL* values of the synthetic *t* and synthetic $\bar{X}$ charts for the cases of estimated ($m \in \{10, 20, 40, 80\}$) and known ($m = +\infty$) process mean or parameterswhen $n = 5$. When $\delta = 0$ and $\tau = 1.0$, four randomly chosen synthetic *t* and synthetic $\bar{X}$ charts' parameter combinations (*K*, *L*), which have the in-control *ARL*, $ARL_0 = 370.4$ when $n = 5$, for the case of known process mean or parameters, are presented in the upper part of each case in Table 1. The optimal-parameter combinations (*K*, *L*) corresponding to the synthetic *t* and synthetic $\bar{X}$ charts with known process mean or parameters, for aspecified δ, $\tau = 1.0$, $ARL_0 = 370.40$ and $n = 5$, are listed in the lower part of each case in Table 1. Readers are encouraged to refer to Calzada and Scariano (2013) and Zhang et al. (2011) for the optimization algorithms of the synthetic *t* and synthetic $\bar{X}$ charts with known process mean or parameters, respectively. The *ARL* and *SDRL* of the synthetic *t* and synthetic $\bar{X}$ charts, for both the cases of known and estimated process mean or parameters, can be determined using the Markov chain method discussed in Section 3 and Zhang et al. (2011), respectively. It should be noted that the (*ARL*, *SDRL*) values in columns three to seven are computed using the specified (*K*, *L*) combination in the second column of Table 1. For example, if $\delta = 1.0$, the optimal-parameter combination ($K = 3.28137$, $L = 3$) of the synthetic *t* chartwith known process mean is used to compute the zero-state ($ARL_1 = 5.66$, $SDRL_1 = 7.45$) when $m = 20$. Here, $SDRL_1$ refers to the out-of-control *SDRL*.

[Insert Table 1 here.]

From Table 1, it is clear that for small mean shifts $(\delta \le 0.6)$ and small *m*, the difference between the (*ARL*, *SDRL*) values of the synthetic $\bar{X}$ chart for known- and estimated-process-parameters cases is significantly larger compared to that of the synthetic *t* chart. For instance, when $\delta = 0.2$ and $m = 10$, the zero- and steady-state (ARL_1, $SDRL_1$) of the synthetic $\bar{X}$ chart are (789.72, 20095.03) and (509.12, 6365.66), respectively (see Table 1). These zero- and steady-state (ARL_1, $SDRL_1$) values decrease to (127.76, 167.16) and (149.17, 147.38), respectively, for $m = +\infty$. From this example, the percentage of differences are (518.13%, 11921.43%) and (241.30%, 4219.22%) corresponding to the zero- and steady-state (*ARL*, *SDRL*). On the other hand, for the same $\delta = 0.2$, the zero- and steady-states (ARL_1, $SDRL_1$) of the synthetic *t* chart for $m = 10$ are (214.95, 299.96) and (222.39, 261.21), respectively; whereas, when $m = +\infty$, the corresponding zero- and steady-state values are (212.18, 256.48)

and (222.14, 221.30), respectively (see Table 1). From this example, the percentage of differences are (1.31%, 16.95%) and (0.11%, 18.03%) corresponding to the zero- and steady-state (*ARL*, *SDRL*). This indicates that the synthetic $\bar{X}$ chart is more seriously affected by estimation errors compared to the synthetic *t* chart.

From Table 1, for both the zero- and steady-state cases, we notice that for a specified shift δ, when *m* increases, the difference between the (*ARL*, *SDRL*) values of the synthetic *t* chart with known- and estimated-process-mean cases decreases. This difference is large for $\delta = 0$, small and moderate shifts $(\delta \le 1)$; while this difference becomes almost negligible for large mean shifts $(\delta \ge 1.5)$. Specifically, when $\delta = 0$, the (ARL_0, $SDRL_0$) values for the cases of estimated process mean increase and approach those of the case of known process mean as *m* increases; while the trend is opposite, i.e. the (ARL_1, $SDRL_1$) values for the cases of estimated process mean decrease and approach those of the case of known process mean when $\delta \ge 0.4$ as *m* increases (see Table 1). Since $\delta = 0.2$ is between $\delta = 0$ and $\delta \ge 0.4$, the ARL_1 trend for $\delta = 0.2$ is fluctuating between the trends for both $\delta = 0$ and $\delta \ge 0.4$. Hence, there is no specific trend in the ARL_1 values for $\delta = 0.2$ as *m* increases.

We further observe from Table 1 that when the process mean μ_0 is estimated, the zero- and steady-state ARL_0 values of the synthetic *t* chart are not equal to the desired ARL_0 value (i.e. 370.40), but they are smaller. This indicates an increased false alarm rate for the case with estimated process mean, which is absolutely unfavorable from the practitioner's point of view. For instance, when *m* = 10, the zero-state $ARL_0 \approx 297$ and the steady-state $ARL_0 \approx 301$, for the synthetic *t* chart (see Table 1). As *m* increases, the ARL_0 becomes closer to 370.40. This example shows the unsuitability of the use of the optimal-parameter combinations (*K*, *L*) corresponding to the case of known process mean in place of that for the case of estimated process mean, for the synthetic *t* chart. In order to obtain the desired performance as the known-process-mean chart, a very large number of *m* (> 80) is required.

The results in Table 1 show that the optimal-parameter combinations (*K*, *L*) of the synthetic *t* chart corresponding to the case of known process mean are inappropriate to be used in the case of estimated process mean, unless *m* is very large. Using these inappropriate values of (*K*, *L*) will lead to unfavourable performance for the synthetic *t* chart with estimated process mean. Besides, collecting a large number of Phase-I samples is usually economically infeasible and time consuming. In some manufacturing processes, the production run is finite and the SPC monitoring should be initiated as early as possible. Therefore, taking a large number of *m* is impractical. For these reasons, in the next Section, we recommend the use of

new optimal-parameter combinations (K, L), specially accounting for parameter estimation and the number of m used in practice.

5. Optimal designs of the synthetic *t* chart with estimated process mean

This section discusses two optimal design strategies for the synthetic t chart by taking process mean estimation into consideration. The two proposed optimal strategies include sensitizing the detection of (i) a specific mean shift and (ii) a range of mean shifts. Accordingly, the proposed two optimization algorithms involve minimizing the zero- and steady-state (i) $ARL_1\left(\delta^*, \tau^*\right)$, as well as (ii) $EARL_1$. Here, $ARL_1\left(\delta^*, \tau^*\right)$ represents the ARL_1 value for a desired mean shift (δ^*) and process variance shift (τ^*), for which a quick detection is required. The four optimization programs are developed using the ScicosLab software (www.scicoslab.org). With these developed optimization programs, practitioners can easily design and implement the synthetic t chart for their desirable requirements, when the process mean is estimated.

5.1. ARL optimization for the synthetic t chart with estimated process mean

If the shift size is known a priori, the new optimal-parameter combination (K, L) of the synthetic t chart with estimated process mean can be determined, in order to

$$\underset{K,\,L}{\text{Minimize}}\; ARL_1\left(\delta^*, \tau^*\right), \tag{20}$$

subject to the constraint

$$ARL_0 = \varepsilon, \tag{21}$$

where ε is the desired in-control ARL value. Using the optimization model (20)-(21), the optimal-parameter combination (K, L) of the synthetic t chart with estimated process mean under both the zero- and steady-state cases, can be obtained by using the following algorithms and pseudo codes:

Set values of m, n, $ARL_0 = \varepsilon$, δ^* and τ^*.
$ARL_1 = +\infty$
$L_1 = 1$
while (true)
    find K_1 that satisfies $ARL\ (m, n, K_1, L_1, \delta = 0, \tau = 1) = ARL_0 = \varepsilon$
    $ARL_\delta = ARL\ (m, n, K_1, L_1, \delta^*, \tau^*)$
    if $ARL_\delta > ARL_1$ then
        break
    else
        $L = L_1$

$K = K_1$
$ARL_1 = ARL_\delta$
$L_1 = L_1 + 1$
end
end

More precisely, the steps involved are described as follows:

Step 1. Specify the desired *m*, *n*, ε, δ^* and τ^* values.

Step 2. Initialize *L* as 1.

Step 3. Search *K* by means of a nonlinear equation solver, in order to fulfil constraint (21), i.e. $ARL_0 = \varepsilon$.

Step 4. Compute the $ARL_1\left(\delta^*, \tau^*\right)$ value for the current values of *L* and *K*.

Step 5. If $L = 1$, increase *L* by one and go back to Step 3. If $L \geq 2$, compare the $ARL_1\left(\delta^*, \tau^*\right)$ value for the current *L* with that of $L-1$. If the current *L* gives a smaller $ARL_1\left(\delta^*, \tau^*\right)$ value, increase *L* by one and go back to Step 3; otherwise, proceed to Step 6.

Step 6. Take the unique combination (*K*, *L*) that gives the smallest $ARL_1\left(\delta^*, \tau^*\right)$ as the optimal chart's parameters of the synthetic *t* chart with estimated process mean.

Note that the stopping criterion in Step 5 can guarantee that the resulting (*K*, *L*) combination is an optimal solution for specific *m*, *n*, ε, δ^* and τ^* values. Huang and Chen (2005), Khoo et al. (2011), and Wu and Spedding (2000) also adopted a similar stopping criterion to that in Step 5 for their proposed synthetic-type charts.

Tables 2 and 3 show the zero- and steady-state (ARL_1, $SDRL_1$) and the optimal-parameter combinations (*K*, *L*) of the synthetic *t* chart corresponding to different combinations of (*m*, *n*, δ^*, $\tau^* = 1.0$). The ARL_0 is set as 370.40 for all entries in Tables 2 and 3. For each δ^*, the optimal-parameter combination (*K*, *L*) is presented in the first row of each cell; while the corresponding (ARL_1, $SDRL_1$) values are listed in the second row of each cell. For instance, in Table 2, when *m* = 40, *n* = 3, $\delta^* = 0.6$ and $\tau^* = 1.0$, the zero-state (ARL_1 = 102.51, $SDRL_1$ = 124.27) and steady-state (ARL_1 = 108.26, $SDRL_1$ = 115.68) are computed using the optimal-parameter combinations (*K* = 5.66309, *L* = 3) and (*K* = 4.20691, *L* = 1), respectively.

[Insert Tables 2 and 3 here.]

From Tables 2 and 3, we notice that for a specified combination (*n*, δ^*), *L* is almost the same for different *m* values; while for a fixed *m*, *L* decreases as δ^* increases. The (ARL_1, $SDRL_1$) values for the estimated-process-mean case are becoming closer to those of the known-process-mean case as *m* increases. It is expected that for small and moderate mean

shifts $\left(\delta^* \le 1.0\right)$, the ($ARL_1$, $SDRL_1$) values for the estimated-process-mean chart are larger than those of the known-process-mean chart, unless when m is large ($m \ge 80$). The difference in the (ARL_1, $SDRL_1$) values between the estimated- and know-process-mean charts becomes almost negligible for large mean shifts $\left(\delta \ge 1.5\right)$.

5.2. EARL optimization for the synthetic t chart with estimated process mean

It is quite common in practice that the shift size is unknown. If a particular shift size is selected to establish a control chart, and the actual shift size is different from that used in the design of the control chart, the run-length properties of the corresponding chart may be adversely affected. For instance, if $n = 5$, $m = 10$, $\delta^* = 1.0$ and $\tau^* = 1.0$, Table 2 gives the optimal chart's parameters ($K = 3.55529$, $L = 4$) of the synthetic *t* chart with estimated process mean under the zero-state case. If the actual shift is $\delta = 0.2$, the zero-state ($ARL_1 = 269.04$, $SDRL_1 = 348.14$) values are obtained with this selected pair of ($K = 3.55529$, $L = 4$) as compared to the zero-state ($ARL_1 = 267.63$, $SDRL_1 = 366.84$) values obtained with the correct pair of optimal parameters ($K = 4.31365$, $L = 15$) (see Table 2). Unlike the first type of optimal design discussed in Section 5.1, the second type (presented in this section) considers the unknown shift size. This optimal design will result in an excellent overall performance over a range of shifts.If the shift size is unknown, the new optimal-parameter combination (K, L) of the synthetic *t* chart with estimated process mean can be computed, in order to

$$\underset{K,\,L}{\text{Minimize}}\, EARL_1, \tag{22}$$

subject to the constraint

$$EARL_0 = \varepsilon, \tag{23}$$

where ε is the desired in-control expected *ARL* ($EARL_0$). The *EARL* can be computed as follows:

$$EARL = \int_{\delta_{\min}}^{\delta_{\max}} ARL\, f_\delta(\delta)\, d\delta, \tag{24}$$

where $f_\delta(\delta)$ is the pdf of δ, while $\delta_{\min}$ and $\delta_{\max}$ are the minimum and maximum values of the mean shifts, respectively. If the practitioners have no prior knowledge about $f_\delta(\delta)$, Castagliola et al. (2011), Ou et al. (2011) and Calzada and Scariano (2013) suggested choosing a uniform distribution over the shift interval $\left[\delta_{\min},\ \delta_{\max}\right]$. Note that other

distributions can also be selected based on the practitioners' specific insight on the process being monitored. In this paper, we use a uniform distribution over [0.1, 2] to compute the zero- and steady-state *EARL* values. The zero- and steady-state *EARL* values are computed with Eq. (24) by using the corresponding zero- and steady-state *ARL* values, respectively. Using the optimization model (22)-(23), the optimal-parameter combination (*K*, *L*) of the synthetic *t* chart with estimated process mean under both the zero- and steady-state cases, can be obtained as follows:

Step 1. Specify the desired *m*, *n*, ε, $\delta_{\min}$, $\delta_{\max}$ and τ^* values.

Step 2 – Step 6. Similar to the optimal design in Section 5.1 but replace constraint (21) with constraint (23), and compute $EARL_1$ instead of $ARL_1\left(\delta^*, \tau^*\right)$.

Note that the optimization model (22)-(23) employs similar algorithms and pseudo codes to that explained in Section 5.1, in which the *ARL* is replaced by *EARL*.

Table 4 presents the unique optimal-parameter combinations (*K*, *L*), the zero- and steady-state $EARL_1$s of the synthetic *t* chart for different *m* and *n* values. All the optimal-parameter combinations in Table 4 must attain an $EARL_0$ of 370.40. Furthermore, $\tau^* = 1.0$ and $\delta \sim U$ [$\delta_{\min} = 0.1$, $\delta_{\max} = 2.0$] are considered. Note that for all *m* and *n* combinations, the synthetic *t* chart gives the smallest $EARL_1$ values by using the corresponding optimal pairs (*K*, *L*). For example, for the zero-state case when $m = 20$ and $n = 7$, the optimal pair ($K = 3.37000$, $L = 11$) results in $EARL_1 = 29.61$. From Table 4, for both the zero- and steady-state cases, it is obvious that for a specified *n*, the $EARL_1$ values of the estimated-process-mean chart decrease and converge to that of the known-process-mean chart, as *m* increases; while for a fixed *m*, the $EARL_1$ value decreases as *n* increases.

6. A real industrial application

In this section, the proposed optimal synthetic *t* chart with estimated process mean is implemented with some real industrial data collected from a silicon epitaxy process. Silicon epitaxy is normally doped with boron for P-type epitaxy or phosphorus for N-type epitaxy. The real data adopted in this section are the N-type epitaxy provided by a wafer substrate manufacturing company. A proper control of epitaxial thickness uniformity across a wafer is essential for accurately controlling electrical properties and successfully providing a perfect substrate for subsequent device processing.

In this example, the quality characteristic of interest is the measurement of epitaxial layer thickness (in micrometre, μm) across a wafer. The first set of data, which comprise m = 20 samples, each with n = 5 observations, are collected to calibrate the proposed optimal chart (Phase-I). These data are collected at 20 equally spaced time points. The summary statistics of these Phase-I data are listed in columns 1 to 3 of Table 5. The stability of these Phase-I data are checked by means of the Bonferroni-type control chart (Ryan, 2000). The Bonferroni-type adjustment is a simpler alternative to the Phase-I control charts. Ryan (2000) claimed that the Bonferroni-type control chart improves the probability of one or more false alarms of the Shewhart chart to a desired value. Also, the Bonferroni-type adjustment provides an approximate solution and is applicable for any symmetric or non-symmetric distributed charting statistics (Chakraborti et al., 2008). Therefore, it is adopted here to analyze the Phase-I data. Figs. 3(a) and (b) display the Bonferroni-adjusted $\bar{X}$ and S charts, whose control limits are computed as $UCL_{\bar{X}}/LCL_{\bar{X}} = \bar{\bar{X}} \pm Z_{FAP/(2m)}\left(\bar{S}/c_4\right)/\sqrt{n}$ and $UCL_S/LCL_S = \bar{S} \pm Z_{FAP/(2m)}\sqrt{1-c_4^{\,2}}\left(\bar{S}/c_4\right)$, respectively. Here, c_4 is an unbiased constant, Z_ς is the $\left(1-\varsigma\right)100^{\text{th}}$ percentage point of the standard normal distribution, FAP is the false alarm probability, $\bar{\bar{X}} = 14.00533\,\mu\text{m}$ is the sample grand average, and $\bar{S} = 0.13830\,\mu\text{m}$ is the average of the m standard deviations. At each sample number i, the probability of a false alarm is 0.0027; hence, $FAP = 1-\left(1-0.0027\right)^{40} = 0.1025$ set in this example, is the probability of at least one false alarm in 40 samples. It also suggests that each chart gives an overall false-alarm probability of at most 0.1025.

[Insert Table 5, Figures 3(a) and (b) here.]

Figs. 3(a) and (b) demonstrate that the Phase-I data are in-control. Thus, $\hat{\mu}_0 = 14.00533$ μm is calculated from Eq. (10). This $\hat{\mu}_0$ value is used in mean estimation for Phase-II process monitoring. The process engineer has decided to implement the synthetic t chart for the Phase-II process monitoring with ARL_0 = 370.40. According to the process engineer, the critical special causes that lead to an anomalous increase in the process mean are variations in the reactor geometry, flow rates, concentration of chemical species, pressure, and temperature. As a consequence, these variations will lead to an unacceptable thickness or non-uniformity and excessive scrap materials. An increasing shift of δ^* = 0.8 in the process mean should be interpreted as a signal that something is going wrong in the production. If m = 20, n = 5, ARL_0 = 370.40, δ^* = 0.8 and τ^* = 1.0 are of interest, the zero-state optimal chart's

parameters (*K*, *L*) are (3.62323, 5), which give (ARL_1 = 12.68, $SDRL_1$ = 18.24) (see Table 2). This optimal pair (*K*, *L*) will be used for process monitoring in Phase-II. Thus, the control limits of the *t/S* sub-chart are $\widehat{UCL}_t$ / $\widehat{LCL}_t = \pm 3.62323$; while the lower limit of the *CRL/S* sub-chart is *L* = 5.

A second set of data comprises 20 additional samples (i.e. *i* = 21 to 40), each having *n* = 5 observations. These Phase-II data are collected from the silicon epitaxy process after the occurrence of a special cause that increases the process mean. Similarly, these data are collected at 20 equally spaced time points. The summary statistics of these Phase-II data are shown in columns 4 to 8 of Table 5. The plotting statistics $\hat{T}_i$ listed in Table 5 are computed using Eq. (12).

Figs. 4(a) and (b) present the synthetic *t* chart with estimated process mean for monitoring the epitaxial layer thickness across a wafer in the silicon epitaxy process (Phase-II). From Fig. 4(b), the first out-of-control status is signaled at *i* = 31 as *CRL* = 2 < *L* = 5. It is obvious that from Fig. 4(b), the synthetic *t* chart with estimated process mean actually detects three out-of-control situations, i.e. samples *i* = 31, 33 and 34. These out-of-control signals confirm the occurrence of an assignable cause, for which the process engineer has to immediately identify and remove it. According to the process engineer, the root cause for this out-of-control situation is the reactor variation. After the completion of the corrective actions, the process continues to operate in the in-control situation again (i.e. samples *i* = 35 to 40).

[Insert Figures 4(a) and (b) here.]

7. Performance studies

7.1. The robustness study of the synthetic t chart with estimated process mean

This section investigates the robustness property of the synthetic *t* chart with estimated process mean. We consider the Phase-II process' instability involving the change of the process mean and/or standard deviation. In Fig. 5, the zero-state ARL_1 and $SDRL_1$ of the synthetic $\bar{X}$ (left side) and synthetic *t* (right side) charts with estimated process parameters or mean are plotted for *n* = 5, *m* = 10, $\tau \in \{0.90, 0.95, 1.00, 1.05, 1.10\}$, $\delta \in [0.0, 1.0]$ and ARL_0 = 370.40. Note that both the synthetic $\bar{X}$ and synthetic *t* charts with estimated process parameters and mean, respectively, are optimized for δ^* = 1.0, τ^* = 1.0, i.e. the optimal charting parameters (*K*, *L*) of the corresponding charts are used to compute all the *ARL* and *SDRL* values. Similar plots are shown in Fig. 6, for *m* = 80. Readers are encouraged to refer to Zhang et al. (2011) for the optimization procedure and the related formulae of the synthetic

$\bar{X}$ chart with estimated process parameters; whereas, the optimal chart's parameters of the synthetic *t* chart for $m \in \{10, 80\}$ can be obtained from Table 2.

[Insert Figures 5 and 6 here.]

Similar to the results demonstrated in Calzada and Scariano (2013) for the known-process-mean case, Figs. 5 and 6 show that the synthetic *t* chart is more robust than the synthetic $\bar{X}$ chart against changes in the process standard deviation, when the process parameters are estimated. When there are changes in the process standard deviation during the Phase-II process monitoring, the synthetic $\bar{X}$ chart with estimated process parameters suffers from an increased false alarm rate (when $\tau > 1.00$) or a very large ARL_0 value (when $\tau < 1.00$), resulting in the chart being oversensitive (when $\tau > 1.00$) or insensitive (when $\tau < 1.00$), respectively, to process changes. From Figs. 5 and 6, we observe that the zero-state *ARL* and *SDRL* values of the synthetic $\bar{X}$ chart with estimated process parameters suffer from large variations when $\delta \leq 0.5$. The discrepancy in *SDRL*s of the synthetic $\bar{X}$ chart with estimated process parameters is remarkably larger than that in the *ARL*s, especially for small *m*. Also, the discrepancy in the *ARL*s and *SDRL*s of the synthetic $\bar{X}$ chart decreases as *m* increases. On the other hand, it is clear from Figs. 5 and 6 that the zero-state *ARL* and *SDRL* values of the synthetic *t* chart with estimated process mean experience only very small variations. This implies that the zero-state *ARL* and *SDRL* curves are hardly distinguishable regardless of the values of τ and *m* considered. Similar results are obtained for other combinations of (*m*, *n*) and those under the steady-state condition. These results can be obtained from the corresponding author.

7.2. Comparative studies

This section compares the *ARL* (left side) and *SDRL* (right side) profiles of the *t*, $\bar{X}$, synthetic *t* and synthetic $\bar{X}$ charts with estimated process mean or parameters, when the process standard deviation is in-control, i.e. $\tau = 1.00$ (see Fig. 7) and unstable, i.e. $\tau \in \{0.9, 1.1\}$ (see Figs. 8 and 9). Note that in Figs. 7 to 9, the word "synthetic" is represented by "syn". Only the *t* chart and its corresponding $\bar{X}$ chart are considered in these comparative studies. This is because only the *t* chart with estimated process mean is proposed in the existing literature (see Castagliola et al., 2013a) and other *t*-type control charts are not yet investigated under the estimated-process-mean case. The zero-state *ARL* and *SDRL* curves of the *t*, $\bar{X}$, synthetic *t* and synthetic $\bar{X}$ charts in Figs. 7 to 9, are plotted for $n = 5$ and $m \in \{20,$

40, 80, +∞}. Furthermore, ARL_0 = 370.40 (i.e. when δ = 0 and τ = 1.0) are considered in these three figures. The *t* and $\bar{X}$ charts' parameters used in Figs. 7 to 9 can be obtained from Castagliola et al. (2013a); while that of the synthetic *t* and synthetic $\bar{X}$ charts are optimized for δ^* = 1.0 (moderate shift) and τ^* = 1.0. The optimal chart's parameters of the synthetic *t* chart with known and estimated process mean can be obtained from Table 2; while that of the synthetic $\bar{X}$ chart can be acquired from Zhang et al. (2011).

[Insert Figures 7, 8 and 9 here.]

It is shown in Fig.7 that the synthetic *t* chart outperforms the *t* chart with known and estimated process mean, for all levels of shifts. In terms of the zero-state *ARL*, the synthetic $\bar{X}$ chart with known and estimated process parameters outperforms all the three competing charts (see Fig. 7). This phenomenon is expected as the $\bar{X}$ -type charts always have the best performance when the process standard deviation is in-control, i.e. τ = 1.0 and the charts' parameters are optimized with respect to small and moderate shifts (see Zhang et al., 2009; Calzada and Scariano, 2013; Sitt et al., 2014). However, for the case of estimated process parameters or mean, although all the four control charts attain the same ARL_0 value irrespective of the value of *m* used, both the $\bar{X}$ and synthetic $\bar{X}$ charts suffer from larger *SDRL*s compared to the *t* and synthetic *t* charts for $\delta \leq 0.3$, especially when *m* is small. This indicates that there is a significantly larger variation of the run-length distribution for the $\bar{X}$ and synthetic $\bar{X}$ charts with estimated process parameters and this variation decreases as *m* increases.

Similar plots are shown in Fig. 8 for the decreasing process standard deviation (τ = 0.90). It can be seen that the synthetic *t* chart with known and estimated process mean is the best among all the four competing charts, in terms of *ARL*s and *SDRL*s; whereas the synthetic $\bar{X}$ chart with known and estimated process parameters is the worst. The $\bar{X}$ and synthetic $\bar{X}$ charts have increased (ARL_0, $SDRL_0$) values and these values decrease as *m* increases. These increased (ARL_0, $SDRL_0$) values make the $\bar{X}$ and synthetic $\bar{X}$ charts with known and estimated process parameters to be insensitive toward the detection of small process mean shifts. Also, the (ARL_1, $SDRL_1$) values of the $\bar{X}$ and synthetic $\bar{X}$ charts with known and estimated process parameters decrease as *m* increases. On the contrary, the (ARL_0, $SDRL_0$) values of the *t* and synthetic *t* charts with known and estimated process mean are always around 370 (see Fig. 8). Moreover, in Fig. 8, the (ARL_1, $SDRL_1$) values of the *t* and synthetic *t*

charts with known and estimated process mean are quite stable regardless of the value of *m* used.

Fig. 9 shows the zero-state *ARL* and *SDRL* plots for the case of an increasing process standard deviation (τ = 1.10). It can easily be noticed that both the $\bar{X}$ and synthetic $\bar{X}$ charts with known and estimated process parameters suffer from increased false alarm rates, which result in oversensitivity in detecting process changes and low *SDRL* values. Since a process is usually in the in-control state for most of the time, it is undesirable to have a high false alarm rate in the context of SPC. Excessive time will be wasted to identify the non-existent assignable cause(s). As a result, practitioners may ignore the implementation of a control chart and conclude that the SPC program is a costly failure. From Fig. 9, the ARL_0 of the *t* and synthetic *t* charts with known and estimated process mean is around 370, irrespective of the value of *m* used. Even though the *t* and synthetic *t* charts with known and estimated process mean are slower in detecting process mean shifts than their $\bar{X}$ -type chart counterparts, the advantage of the two former charts in the in-control state outweighs the high false alarms of the $\bar{X}$ and synthetic $\bar{X}$ charts.

Similar results and conclusions are obtained for other combinations of (m, n, δ, τ) under both the zero- and steady-state conditions. These results can be acquired from the corresponding author upon request. In Figs. 7 to 9, we can conclude that the $\bar{X}$ -type charts with known and estimated process parameters are significantly affected by instability or estimation errors in the in-control standard deviation. The *t*-type charts with known and estimated process mean are very robust against changes in τ and the choice for *m*. Note that the accuracy of all the theoretical results in this paper has been successfully validated via Monte Carlo simulation with 100,000 simulation trials. This Monte Carlo simulation is written in the Statistical Analysis System (SAS) software.

8. Conclusions

In this paper, the synthetic *t* chart with estimated process mean is proposed. The statistical properties (pmf, cdf, *ARL* and *SDRL*) of the synthetic *t* chart with estimated process mean are derived using a Markov chain approach. Two optimal design strategies for the synthetic *t* chart with estimated process mean are developed in this paper. The developed optimization algorithms involve minimizing the ARL_1 and $EARL_1$, for known and unknown shift sizes, respectively. The user-specified ARL_0 and $EARL_0$ can be attained with the application of the proposed optimal designs of the synthetic *t* chart with estimated process

mean; while maintaining a preferable chart performance, as compared with that of the known-process-mean case.

To facilitate the implementation of the proposed control chart in practice, new optimal chart's parameters for both the deterministic and unknown shift-size conditions are provided for practitioners. The optimal chart's parameters for the latter condition are particularly useful especially when practitioners lack of knowledge regarding the shift size and have insufficient historical data regarding the process being monitored. To avoid the misspecification of the chart's statistical performance, the new optimal chart's parameters for the synthetic *t* chart with estimated process mean are obtained by accounting for parameter estimation, as well as practical *m* and *n* values, which can be easily adopted in industries.

This paper also shows that when the process mean or parameters are estimated in Phase-I and there are changes in the process standard deviation in Phase-II, the synthetic *t* chart is more robust than the synthetic $\bar{X}$ chart. The synthetic $\bar{X}$ chart with known and estimated process parameters encounters an increased false alarm rate (when $\tau > 1.0$) or insensitivity in detecting small mean shifts (when $\tau < 1.0$). These disadvantages are larger for small *m*. Furthermore, though the synthetic $\bar{X}$ chart with estimated process parameters outperforms the synthetic *t* chart with estimated process mean when the process standard deviation is in-control ($\tau = 1$), it suffers from tremendously large *SDRL*s, especially when *m* is small.

Since only the *t* (see Castagliola et al., 2013a) and the synthetic *t* (see this paper) charts with estimated process mean are proposed in the literature, more research works need to focus on the adaptive *t*-type, EWMA *t* and CUSUM *t* charts with estimated process mean. Also, the *t*-type control charts are suitable to be implemented in short production runs (see Castagliola et al., 2013a, b; Celano et al., 2013). Therefore, it is worthwhile to investigate the truncated *ARL* and *SDRL* of *t*-type control charts with estimated process mean in short production runs. The proposed synthetic *t* chart with estimated mean in this paper requires the assumption of a normal underlying distribution; thus, its performance under non-normal distribution deserves a future investigation.

Acknowledgements

This research is supported by the Universiti Tunku Abdul Rahman, Fundamental Research Grant Scheme (FRGS), no. FRGS/1/2015/SG04/UTAR/02/3.

Appendix A. Derivation of $\hat{p}$ in Eq. (15)

Let $Y_{i,j}$ be a Phase-II observation obtained at the i^{th} subgroup, where each subgroup contains n observations, for $j = 1, 2, \ldots, n$. Assume that $Y_{i,j}$ follows an independent and identically distributed normal, $N(\mu_0+\delta\sigma_0, \tau^2\sigma_0^2)$ distribution. The random variable $\hat{T}_i$ in Eq. (12) can be transformed into

$$\hat{T}_i = \frac{Z_i + \hat{\lambda}}{\sqrt{\frac{W_i}{n-1}}}, \text{ for } i = 1, 2, \ldots, \tag{A.1}$$

which follows a non-central Student's t distribution with non-centrality parameter $\hat{\lambda}$ and $n-1$ degrees of freedom. The random variables Z_i and W_i in Eq. (A.1) are related to the following fundamental distributions:

$$Z_i = \frac{\left(\bar{Y}_i - \mu_0 - \delta\sigma_0\right)\sqrt{n}}{\tau\sigma_0} \sim N(0,1) \tag{A.2}$$

and

$$W_i = \frac{(n-1)S_i^2}{\tau^2\sigma_0^2} \sim \chi^2(n-1), \tag{A.3}$$

where S_i^2 denotes the i^{th} sample variance involving observations $Y_{i,j}$, for $j = 1, 2, \ldots, n$; while the notation $\chi^2(n-1)$ represents the Chi-square distribution with $n-1$ degrees of freedom. Then the non-centrality parameter $\hat{\lambda}$ in Eq. (A.1) can be obtained as

$$\hat{\lambda} = \frac{\left(\mu_0 - \hat{\mu}_0 + \delta\sigma_0\right)\sqrt{n}}{\tau\sigma_0}. \tag{A.4}$$

Let the random variable U be defined as

$$U = \left(\mu_0 - \hat{\mu}_0\right)\frac{\sqrt{n}}{\sigma_0}. \tag{A.5}$$

Since $\mu_0 - \hat{\mu}_0 \sim N\left(0,\ \sigma_0^2/mn\right)$, then U follows a normal, $N\left(0,\ 1/m\right)$ distribution. The pdf of U is then deduced as

$$f_U\left(u|m\right) = \phi\left(u\middle|0,\ \frac{1}{m}\right), \tag{A.6}$$

where $\phi(\cdot)$ is the pdf of the normal $\left(0,\ 1/m\right)$ distribution. Hence, the $\hat{\lambda}$ in Eq. (A.4) can be simplified to

$$\hat{\lambda} = \frac{\delta\sqrt{n} + U}{\tau}. \tag{A.7}$$

The conditional probability $\hat{p} = P\left(\hat{T}_i \notin \left[\widehat{LCL}_t, \widehat{UCL}_t\right] | \hat{\mu}_0\right)$ is equal to

$$\begin{aligned}\hat{p} &= P\left(\hat{T}_i \geq \widehat{UCL}_t | \hat{\mu}_0\right) + P\left(\hat{T}_i \leq \widehat{LCL}_t | \hat{\mu}_0\right) \\ &= 1 - F_t\left(\widehat{UCL}_t \left| n-1, \frac{\delta\sqrt{n}+U}{\tau}\right.\right) + F_t\left(\widehat{LCL}_t \left| n-1, \frac{\delta\sqrt{n}+U}{\tau}\right.\right). \end{aligned} \quad \text{(A.8)}$$

References

Aparisi, F., & de Luna, M. A. (2009). Synthetic- $\bar{X}$ control charts optimized for in-control and out-of-control regions. *Computers & Operations Research*, *36*, 3204–3214.

Calzada, M. E., & Scariano, S. M. (2013). The synthetic *t* and synthetic EWMA *t* charts. *Quality Technology & Quantitative Management*, *10*, 37–56.

Castagliola, P., Celano, G., & Fichera, S. (2013a). Comparison of the $\bar{X}$ chart and the *t* chart when the parameters are estimated. *Quality Technology & Quantitative Management*, *10*, 1–16.

Castagliola, P., Celano, G., Fichera, S., & Nenes, G. (2013b). The variable sample size *t* control chart for monitoring short production runs. *International Journal of Advanced Manufacturing Technology*, *66*, 1353–1366.

Castagliola, P., Celano, G., & Psarakis, S. (2011). Monitoring the coefficient of variation using EWMA charts. *Journal of Quality Technology*, *43*, 249–265.

Castagliola, P., & Maravelakis, P. (2011). A CUSUM control chart for monitoring the variance when parameters are estimated. *Journal of Statistical Planning and Inference*, *141*, 1463–1478.

Castagliola, P., Zhang, Y., Costa, A., & Maravelakis, P. (2012). The variable sample size $\bar{X}$ chart with estimated parameters. *Quality and Reliability Engineering International*, *28*, 687–699.

Celano, G., Castagliola, P., Fichera, S., & Nenes, G. (2013). Performance of *t* control charts in short runs with unknown shift sizes. *Computers & Industrial Engineering*, *64*, 56–68.

Chakraborti, S., Human, S. W., & Graham, M. A. (2008). Phase-I statistical process control charts: an overview and some results. *Quality Engineering*, *21*, 52–62.

Chong, Z. L., Khoo, M. B. C., & Castagliola, P. (2014). Synthetic double sampling *np* control chart for attributes. *Computers & Industrial Engineering*, *75*, 157–169.

Costa, A. F. B., de Magalhães, M. S., & Epprecht, E. K. (2009). Monitoring the process mean and variance using a synthetic control chart with two-stage testing. *International Journal of Production Research*, *47*, 5067–5086.

Costa, A. F. B., &, Machado, M. A. G. (2016). A side-sensitive synthetic chart combined with a VSS $\bar{X}$ chart. *Computers & Industrial Engineering*, *91*, 205–214.

Davis, R. B., & Woodall, W. H. (2002). Evaluating and improving the synthetic control chart. *Journal of Quality Technology*, *34*, 200–208.

Darroch, J. N., & Seneta, E. (1965). On quasi-stationary distributions in absorbing discrete time finite Markov chains. *Journal of Applied Probability*, *2*, 88–100.

Faraz, A., Woodall, W. H., & Heuchenne, C. (2015).Guaranteed conditional performance of the S^2 control chart with estimated parameters. *International Journal of Production Research*, *53*, 4405–4413.

Guo, B., Wang, B. X., & Cheng, Y. (2015). Optimal design of a synthetic chart for monitoring process dispersion with unknown in-control variance. *Computers & Industrial Engineering*, *88*, 78–87.

Haq, A., Brown, J., & Moltchanova, E. (2016a). New synthetic EWMA and synthetic CUSUM control charts for monitoring the process mean. *Quality and Reliability Engineering International*, *32*, 269–290.

Haq, A., Brown, J., & Moltchanova, E. (2016b). A new synthetic exponentially weighted moving average control chart for monitoring process dispersion. *Quality and Reliability Engineering International*, *32*, 241–256.

Huang, H. J., & Chen, F. L. (2005). A synthetic control chart for monitoring process dispersion with sample standard deviation. *Computers & Industrial Engineering*, *49*, 221–240.

Jensen, W. A., Jones-Farmer, L. A., Champ, C. W., & Woodall, W. H. (2006). Effects of parameter estimation on control chart properties: a literature review. *Journal of Quality Technology*, *38*, 349–364.

Kazemzadeh, R. B., Karbasian, M., & Babakhani, M. A. (2013). An EWMA *t* chart with variable sampling intervals for monitoring the process mean. *International Journal of Advanced Manufacturing Technology*, *66*, 125–139.

Khoo, M. B. C., Lee, H. C., Wu, Z., Chen, C. H., & Castagliola, P. (2011). A synthetic double sampling control chart for the process mean. *IIE Transactions*, *43*, 23–38.

Latouche, G., & Ramaswami, V. (1999). *Introduction to Matrix Analytic Methods in Stochastic Modelling*. Philadelphia: ASA SIAM.

Neuts, M. (1981). *Matrix-Geometric Solutions in Stochastic Models: An Algorithmic Approach*. New York: Dover Publications Inc.

Ou, Y., Wu, Z., &Goh, T. N. (2011). A new SPRT chart for monitoring process mean and variance. *International Journal of Production Economics*, *132*, 303–314.

Psarakis, S., Angeliki, K., Vyniou, A. K., & Castagliola, P. (2014). Some recent developments on the effects of parameter estimation on control charts. *Quality and Reliability Engineering International*, *30*, 1113–1129.

Ryan, T. P. (2000). *Statistical Methods for Quality Improvement*. (2nd ed.). New York: John Wiley &Sons.

Sitt, C. K., Khoo, M. B. C., Shamsuzzaman, M., & Chen, C. H. (2014). The run sum *t* control chart for monitoring process mean changes in manufacturing. *International Journal of Advanced Manufacturing Technology*, *70*, 1487–1504.

Teoh, W. L., Khoo, M. B. C., Castagliola, P., & Chakraborti, S. (2014). Optimal design of the double sampling $\bar{X}$ chart with estimated parameters based on median run length. *Computers & Industrial Engineering*, *67*, 104–115.

Wu, Z., Ou, Y., Castagliola, P., & Khoo, M. B. C. (2010). A combined synthetic & *X* chart for monitoring the process mean. *International Journal of Production Research*, *48*, 7423–7436.

Wu, Z., & Spedding, T. A. (2000). A synthetic control chart for detecting small shifts in the process mean. *Journal of Quality Technology*, *32*, 32–38.

Wu, Z., Yeo, S. H., & Spedding, T. A. (2001). A synthetic control chart for detecting fraction nonconforming increases. *Journal of Quality Technology*, *33*, 104–111.

Zhang, Y., Castagliola, P., Wu, Z., & Khoo, M. B. C. (2011). The synthetic $\bar{X}$ chart with estimated parameters. *IIE Transactions*, *43*, 676–687.

Zhang, L., Chen, G., & Castagliola, P. (2009). On *t* and EWMA *t* charts for monitoring changes in the process mean. *Quality and Reliability Engineering International*, *25*, 933–945.

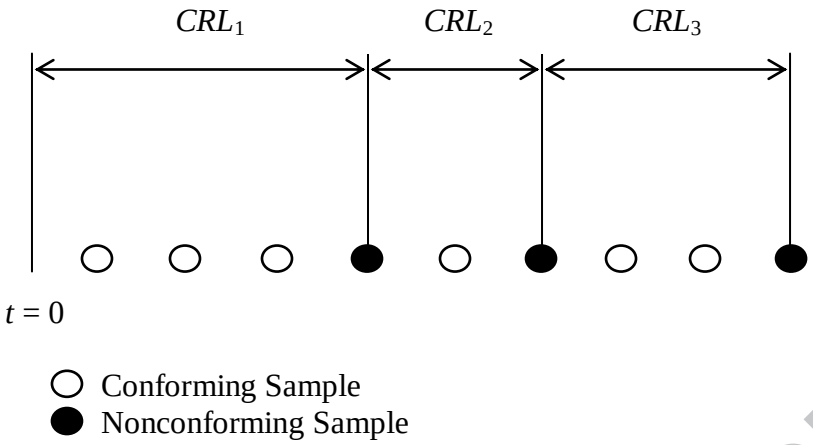

Fig. 1. Conforming run length (*CRL*).

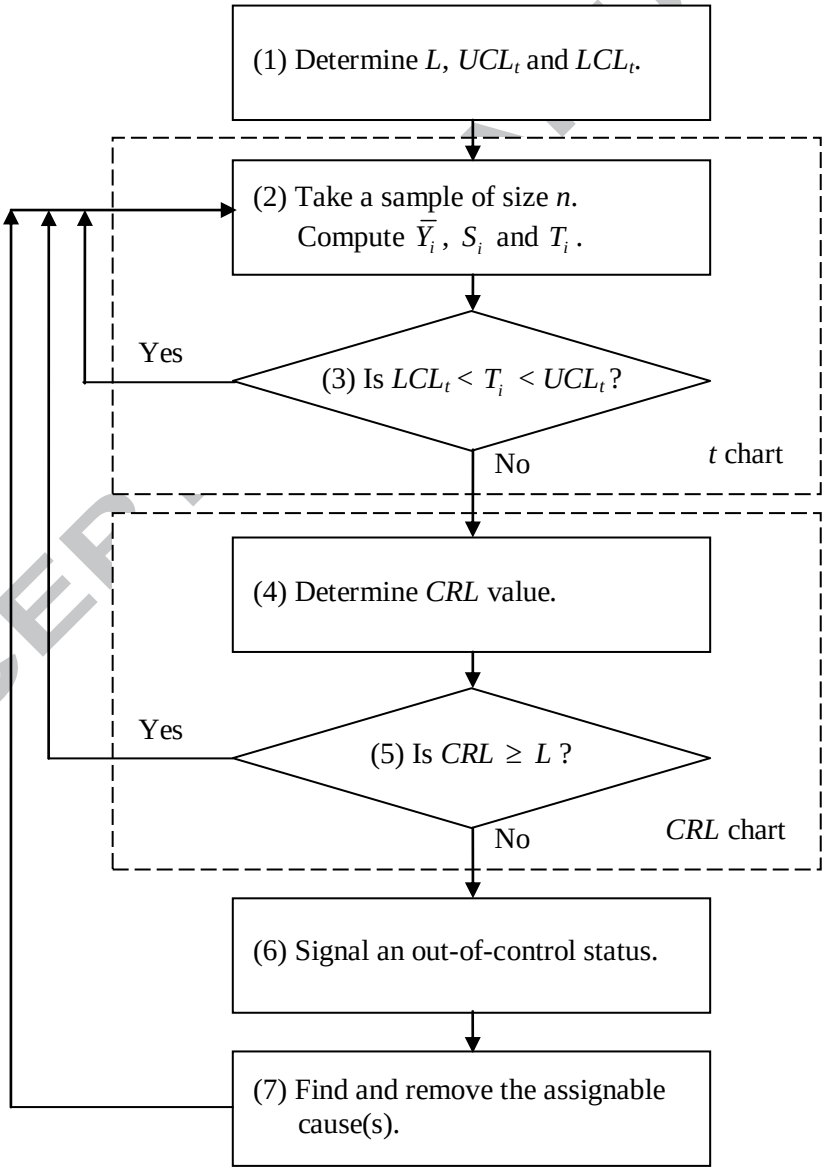

Fig. 2. A flow diagram for the implementation of the synthetic *t* chart.

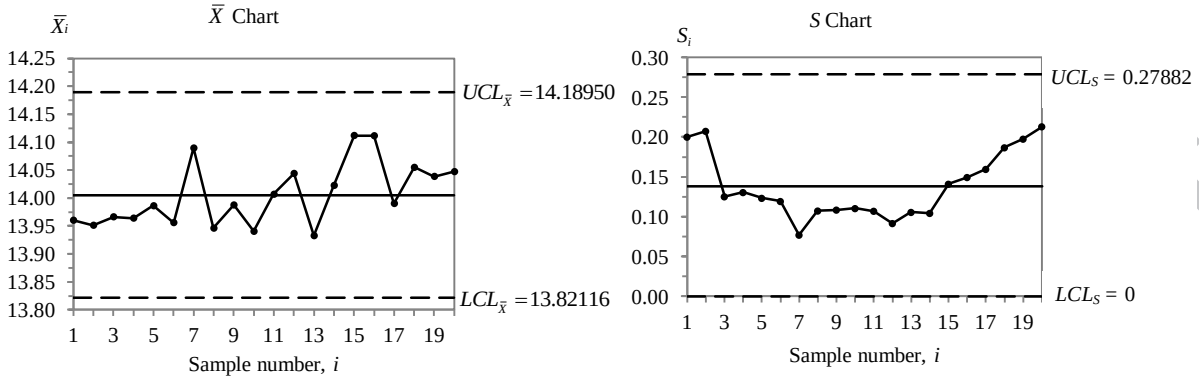

(a) (b)

Fig. 3. The Bonferroni-adjusted (a) $\bar{X}$ and (b) S charts for analysing the Phase-I data.

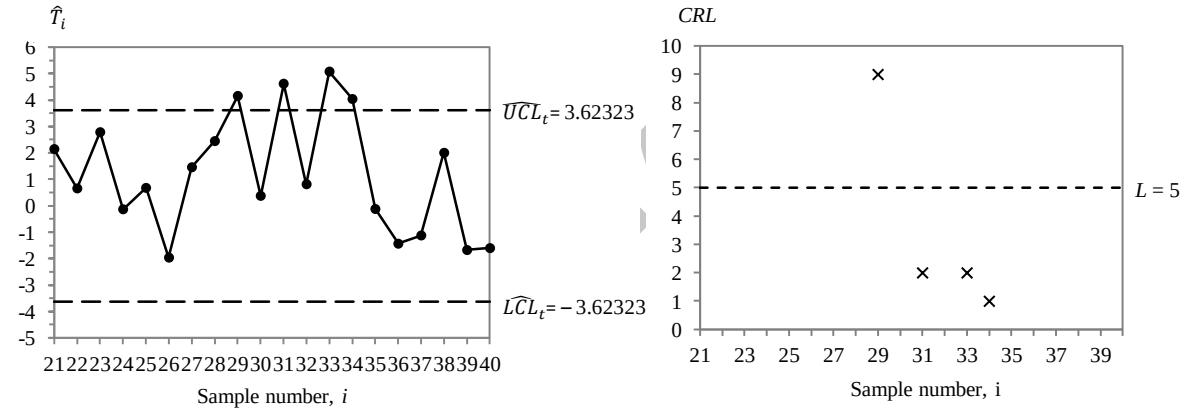

(a) (b)

Fig. 4. The (a) *t/S* and (b) *CRL/S* sub-charts with estimated process mean for monitoring the Phase-II data.

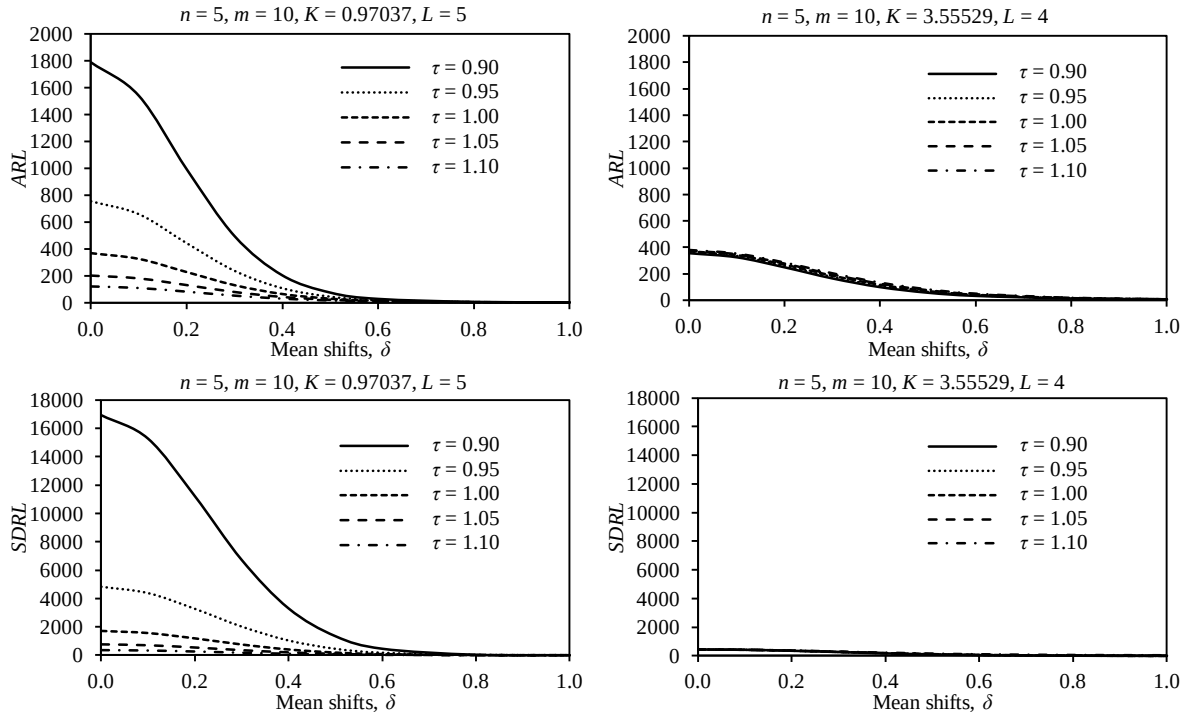

Fig. 5. Zero-state ARL_1 and $SDRL_1$ curves of the synthetic $\bar{X}$ (left side) and synthetic t (right side) charts with estimated process parameters, which are optimized for $\delta^* = 1.0$ and $\tau^* = 1.0$, when $n = 5$, $m = 10$, $\tau \in \{0.90, 0.95, 1.00, 1.05, 1.10\}$ and $ARL_0 = 370.40$.

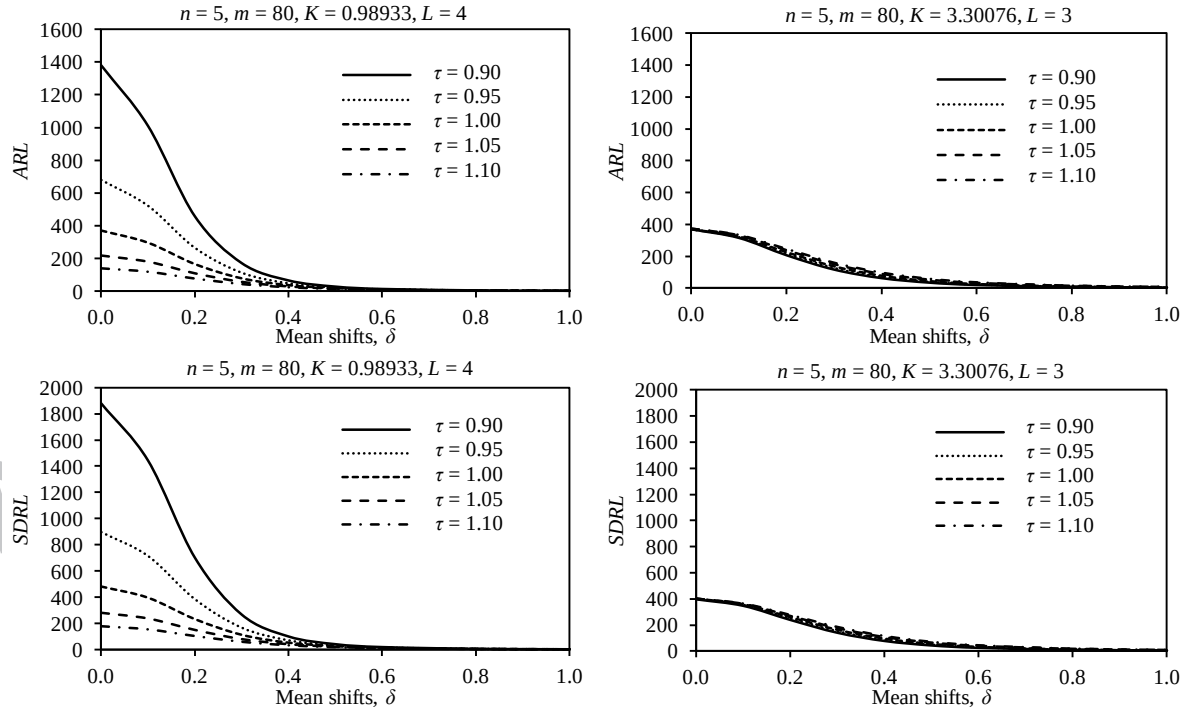

Fig. 6. Zero-state ARL_1 and $SDRL_1$ curves of the synthetic $\bar{X}$ (left side) and synthetic t (right side) charts with estimated process parameters, which are optimized for $\delta^* = 1.0$ and $\tau^* = 1.0$, when $n = 5$, $m = 80$, $\tau \in \{0.90, 0.95, 1.00, 1.05, 1.10\}$ and $ARL_0 = 370.40$.

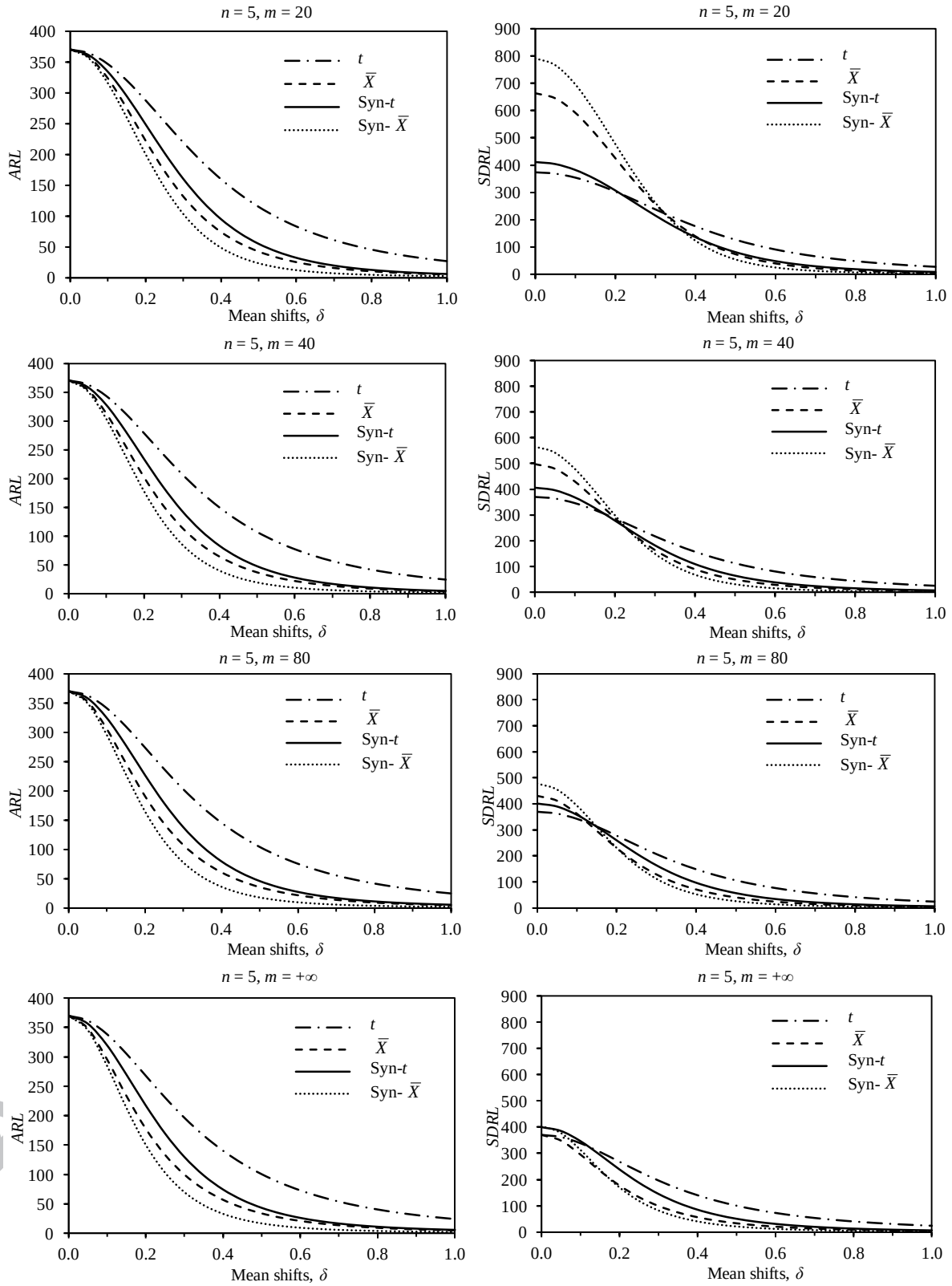

Fig. 7. A comparison of the zero-state *ARL* (left side) and *SDRL* (right side) curves for the *t*, $\bar{X}$, synthetic *t* and synthetic $\bar{X}$ charts, which are optimized for $\delta^* = 1.0$, $\tau^* = 1.0$ and $ARL_0 = 370.40$, when $n = 5$, $m \in \{20, 40, 80, +\infty\}$ and $\tau = 1.0$.

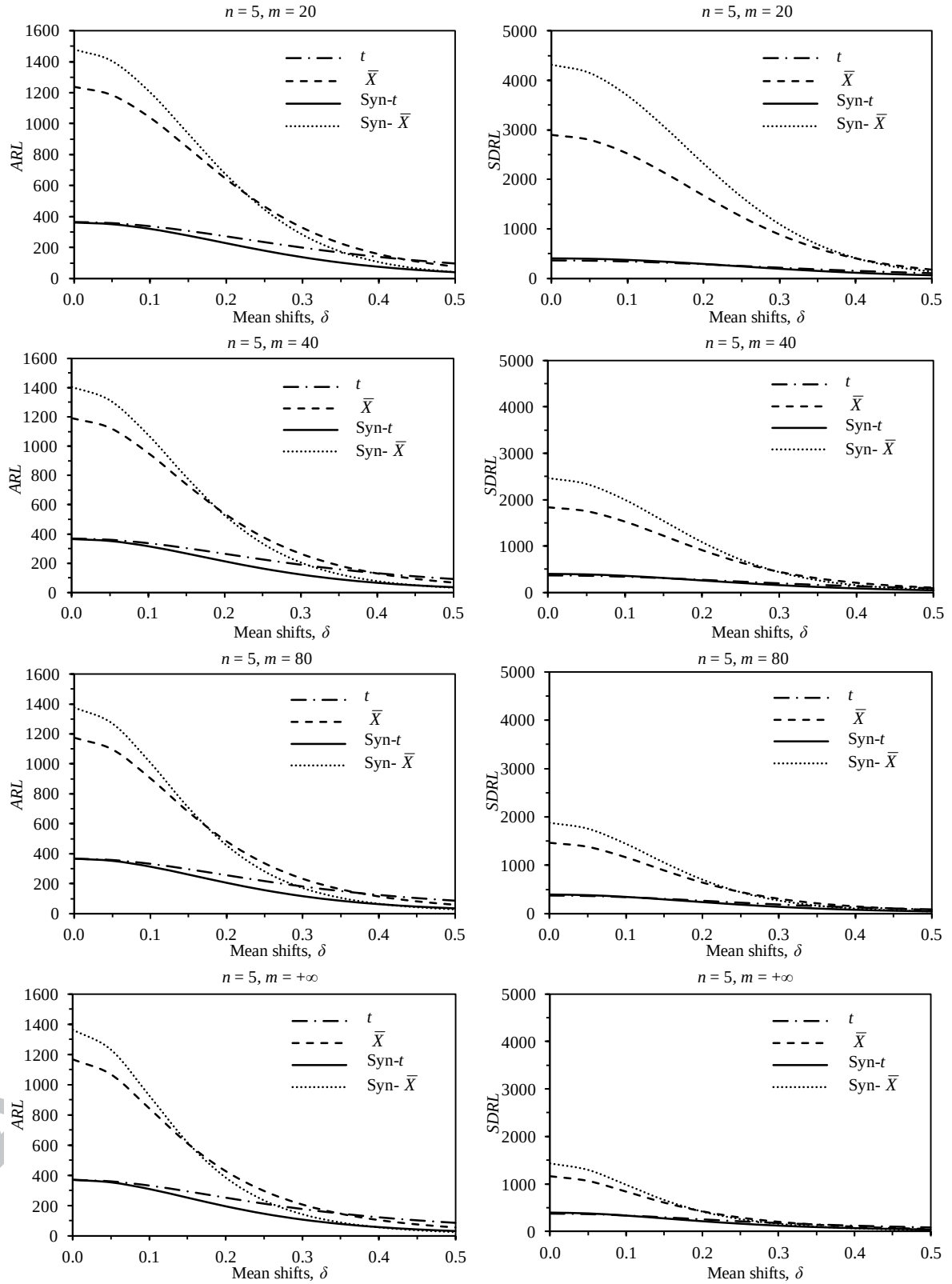

Fig. 8. A comparison of the zero-state *ARL* (left side) and *SDRL* (right side) curves for the *t*, $\bar{X}$, synthetic *t* and synthetic $\bar{X}$ charts, which are optimized for $\delta^* = 1.0$, $\tau^* = 1.0$ and $ARL_0 = 370.40$, when $n = 5$, $m \in \{20, 40, 80, +\infty\}$ and $\tau = 0.9$.

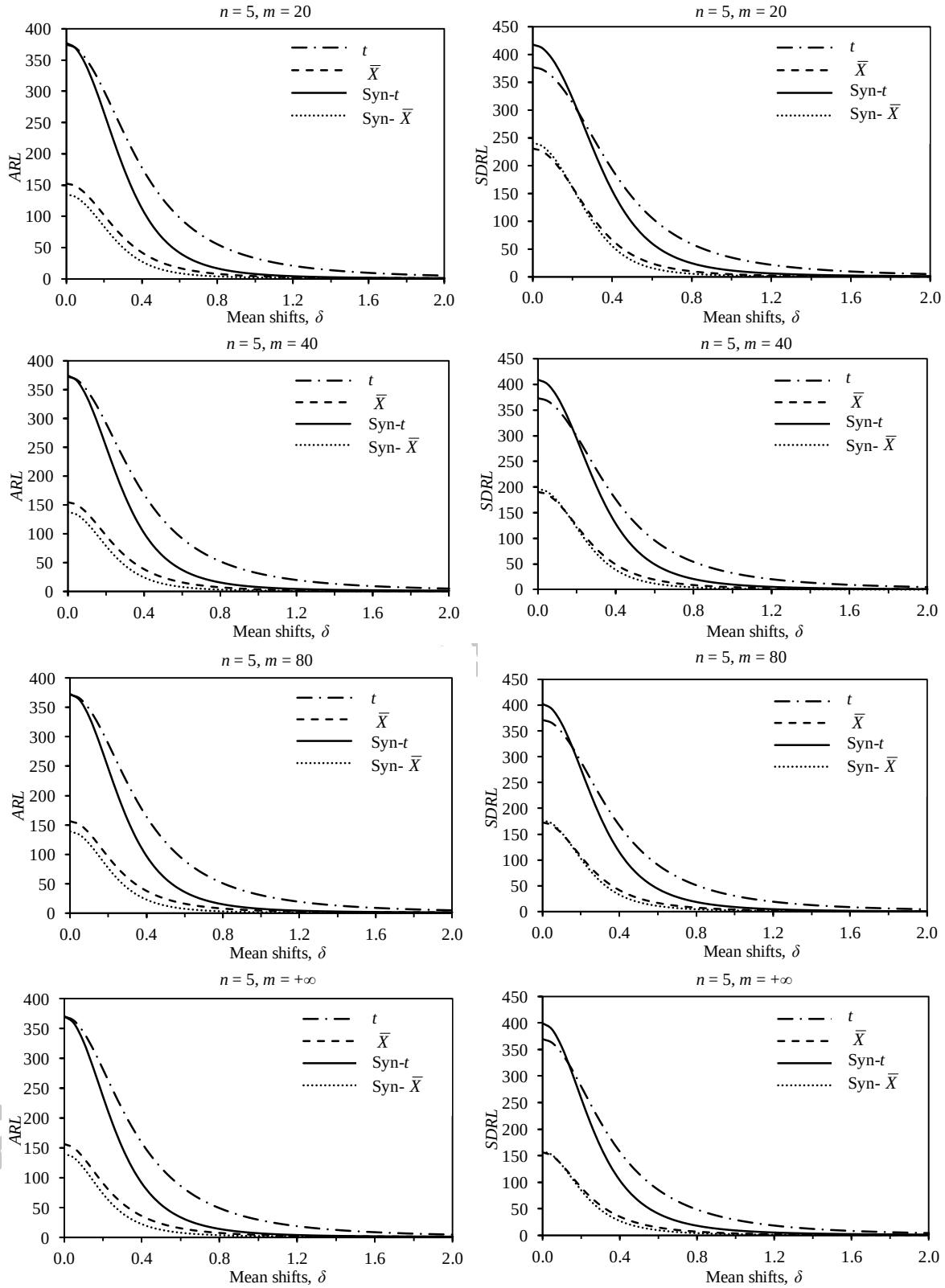

Fig. 9. A comparison of the zero-state *ARL* (left side) and *SDRL* (right side) curves for the *t*, $\bar{X}$, synthetic *t* and synthetic $\bar{X}$ charts, which are optimized for $\delta^* = 1.0$, $\tau^* = 1.0$ and $ARL_0 = 370.40$, when $n = 5$, $m = \{20, 40, 80, +\infty\}$ and $\tau = 1.1$.

Table 1

Zero- and steady-state (*ARL*, *SDRL*) values of the synthetic *t* and synthetic $\bar{X}$ charts when $n = 5$ and $m \in \{10, 20, 40, 80, +\infty\}$ with the optimal charts' parameters (K, L) corresponding to the known-process-parameter case ($m = +\infty$).

		$m = 10$	$m = 20$	$m = 40$	$m = 80$	$m = +\infty$
δ	(K, L)	(*ARL*, *SDRL*)	(*ARL*, *SDRL*)	(*ARL*, *SDRL*)	(*ARL*, *SDRL*)	(*ARL*, *SDRL*)
			Synthetic *t* Chart			
			Zero State			
0.0	(3.43137, 4)	(297.99, 344.15)	(326.73, 364.85)	(345.81, 380.36)	(357.22, 390.61)	(370.40, 403.67)
0.0	(3.55010, 5)	(297.53, 346.79)	(326.40, 367.77)	(345.61, 383.50)	(357.10, 393.89)	(370.40, 407.15)
0.0	(3.73310, 7)	(296.95, 351.29)	(325.98, 372.73)	(345.34, 388.78)	(356.95, 399.39)	(370.40, 412.94)
0.0	(3.93233, 10)	(296.52, 356.77)	(325.66, 378.72)	(345.13, 395.14)	(356.83, 405.99)	(370.40, 419.83)
0.2	(4.30403, 19)	(214.95, 299.96)	(217.21, 290.70)	(216.16, 278.85)	(214.63, 269.39)	(212.18, 256.48)
0.4	(3.98646, 11)	(93.43, 156.09)	(83.07, 124.83)	(77.22, 106.56)	(74.22, 97.36)	(71.22, 88.46)
0.6	(3.73310, 7)	(33.40, 59.88)	(28.83, 43.63)	(26.78, 37.00)	(25.83, 34.13)	(24.92, 31.53)
0.8	(3.55010, 5)	(12.99, 21.73)	(11.60, 16.61)	(10.99, 14.70)	(10.71, 13.87)	(10.45, 13.11)
1.0	(3.28137, 3)	(6.11, 9.02)	(5.66, 7.45)	(5.46, 6.84)	(5.36, 6.56)	(5.27, 6.31)
1.5	(3.07570, 2)	(1.91, 1.89)	(1.86, 1.75)	(1.84, 1.68)	(1.83, 1.65)	(1.82, 1.62)
2.0	(3.07570, 2)	(1.20, 0.61)	(1.19, 0.59)	(1.19, 0.57)	(1.19, 0.56)	(1.18, 0.56)
			Steady State			
0.0	(3.23673, 3)	(301.22, 317.09)	(328.88, 335.38)	(347.11, 349.20)	(357.95, 358.37)	(370.40, 370.08)
0.0	(3.37882, 4)	(300.82, 316.89)	(328.59, 335.23)	(346.91, 349.11)	(357.83, 358.32)	(370.40, 370.13)
0.0	(3.49051, 5)	(300.60, 316.81)	(328.41, 335.17)	(346.79, 349.08)	(357.75, 358.32)	(370.40, 370.18)
0.0	(3.72977, 8)	(300.40, 316.90)	(328.24, 335.29)	(346.68, 349.23)	(357.68, 358.51)	(370.40, 370.43)
0.2	(3.66129, 7)	(222.39, 261.21)	(225.42, 252.37)	(225.05, 241.54)	(224.00, 232.98)	(222.14, 221.30)
0.4	(3.37882, 4)	(102.60, 143.01)	(92.94, 114.45)	(87.41, 97.48)	(84.55, 88.79)	(81.67, 80.27)
0.6	(3.23673, 3)	(40.10, 57.50)	(35.50, 41.99)	(33.41, 35.49)	(32.43, 32.62)	(31.48, 30.01)
0.8	(3.04026, 2)	(17.23, 21.92)	(15.72, 16.76)	(15.06, 14.78)	(14.75, 13.91)	(14.45, 13.11)
1.0	(3.04026, 2)	(8.87, 9.41)	(8.37, 7.80)	(8.14, 7.15)	(8.04, 6.86)	(7.93, 6.59)
1.5	(2.71512, 1)	(3.31, 2.23)	(3.25, 2.07)	(3.23, 2.00)	(3.21, 1.96)	(3.20, 1.93)
2.0	(2.71512, 1)	(2.24, 0.83)	(2.23, 0.80)	(2.22, 0.78)	(2.22, 0.78)	(2.22, 0.77)
			Synthetic $\bar{X}$ Chart			
			Zero State			
0.0	(0.93236, 2)	(534.00, 2074.82)	(422.93, 817.43)	(389.77, 556.13)	(378.21, 465.96)	(370.40, 394.58)
0.0	(0.96779, 3)	(584.31, 2721.93)	(438.61, 918.25)	(396.04, 590.17)	(381.00, 482.59)	(370.40, 399.60)
0.0	(0.99226, 4)	(626.18, 3340.29)	(450.92, 1001.44)	(400.85, 616.70)	(383.10, 495.38)	(370.40, 403.67)
0.0	(1.04906, 8)	(753.40, 5676.22)	(485.01, 1251.17)	(413.77, 689.43)	(388.73, 529.83)	(370.40, 415.43)
0.2	(1.19656, 60)	(789.72, 20095.03)	(288.24, 1345.25)	(189.47, 437.95)	(155.25, 267.38)	(127.76, 167.16)
0.4	(1.12974, 23)	(132.20, 2722.02)	(52.90, 198.93)	(36.89, 73.37)	(31.58, 49.57)	(27.45, 35.42)
0.6	(1.07413, 11)	(21.03, 242.90)	(12.04, 28.06)	(9.89, 15.53)	(9.09, 12.38)	(8.43, 10.15)
0.8	(1.02586, 6)	(5.71, 21.91)	(4.39, 6.88)	(3.98, 5.02)	(3.82, 4.40)	(3.67, 3.91)
1.0	(0.99226, 4)	(2.59, 4.39)	(2.30, 2.58)	(2.19, 2.15)	(2.14, 1.98)	(2.10, 1.83)
1.5	(0.93236, 2)	(1.17, 0.60)	(1.15, 0.51)	(1.13, 0.47)	(1.13, 0.45)	(1.13, 0.43)
2.0	(0.93236, 2)	(1.01, 0.13)	(1.01, 0.11)	(1.01, 0.10)	(1.01, 0.10)	(1.01, 0.09)
			Steady State			
0.0	(0.92599, 2)	(514.51, 1857.56)	(416.08, 755.01)	(386.86, 518.92)	(376.84, 436.16)	(370.40, 369.91)
0.0	(0.98379, 4)	(587.81, 2830.44)	(438.49, 893.64)	(395.76, 560.46)	(380.78, 452.83)	(370.40, 370.04)
0.0	(1.00161, 5)	(615.38, 3266.63)	(446.32, 945.07)	(398.80, 574.63)	(382.13, 458.36)	(370.40, 370.16)
0.0	(1.02774, 7)	(660.58, 4074.15)	(458.45, 1028.76)	(403.40, 596.38)	(384.14, 466.63)	(370.40, 370.32)
0.2	(1.11856, 25)	(509.12, 6365.66)	(260.58, 788.50)	(196.02, 334.33)	(170.90, 223.11)	(149.17, 147.38)
0.4	(1.06143, 11)	(116.06, 1175.35)	(61.67, 153.28)	(47.81, 69.09)	(42.75, 49.21)	(38.59, 36.10)
0.6	(1.01590, 6)	(25.47, 145.76)	(17.36, 27.82)	(15.08, 16.95)	(14.18, 13.83)	(13.41, 11.49)
0.8	(0.98379, 4)	(8.63, 19.48)	(7.20, 7.85)	(6.71, 5.96)	(6.51, 5.28)	(6.32, 4.72)
1.0	(0.96029, 3)	(4.40, 4.96)	(4.05, 3.19)	(3.92, 2.70)	(3.86, 2.50)	(3.80, 2.33)
1.5	(0.92599, 2)	(2.19, 0.82)	(2.17, 0.71)	(2.16, 0.66)	(2.16, 0.64)	(2.15, 0.62)
2.0	(1.34164, +∞)	(1.11, 0.37)	(1.09, 0.33)	(1.08, 0.30)	(1.08, 0.29)	(1.08, 0.29)

Table 2

K, L, ARL_1 and $SDRL_1$ values of the optimal synthetic t chart when $n \in \{3, 5\}$, $m \in \{10, 20, 40, 80, +\infty\}$, $\tau^* = 1.0$ and $ARL_0 = 370.40$ for both zero- and steady-state cases.

	Zero State					Steady State				
	$m = 10$	$m = 20$	$m = 40$	$m = 80$	$m = +\infty$	$m = 10$	$m = 20$	$m = 40$	$m = 80$	$m = +\infty$
δ^*	(K, L) $(ARL_1, SDRL_1)$	(K, L) $(ARL_1, SDRL_1)$	(K, L) $(ARL_1, SDRL_1)$	(K, L) $(ARL_1, SDRL_1)$	(K, L) $(ARL_1, SDRL_1)$	(K, L) $(ARL_1, SDRL_1)$	(K, L) $(ARL_1, SDRL_1)$	(K, L) $(ARL_1, SDRL_1)$	(K, L) $(ARL_1, SDRL_1)$	(K, L) $(ARL_1, SDRL_1)$
$n = 3$										
0.2	(6.25956, 4) (322.05, 376.61)	(6.15208, 4) (313.26, 357.61)	(6.09003, 4) (307.20, 345.12)	(6.05616, 4) (303.52, 337.56)	(6.01989, 4) (299.26, 328.69)	(4.32507, 1) (323.53, 346.52)	(5.06451, 2) (315.17, 328.54)	(5.01324, 2) (309.42, 316.78)	(4.98529, 2) (305.94, 309.68)	(4.95538, 2) (301.90, 301.36)
0.4	(5.82088, 3) (218.70, 279.60)	(5.72083, 3) (200.56, 243.87)	(6.09003, 4) (189.72, 224.36)	(6.05616, 4) (183.76, 212.08)	(6.01989, 4) (177.41, 199.02)	(4.32507, 1) (222.70, 260.99)	(4.25006, 1) (205.32, 227.26)	(4.20691, 1) (194.93, 206.39)	(4.18341, 1) (189.23, 194.79)	(4.15833, 1) (183.16, 182.42)
0.6	(5.82088, 3) (126.35, 176.42)	(5.72083, 3) (110.69, 141.93)	(5.66309, 3) (102.51, 124.27)	(5.63158, 3) (98.36, 115.59)	(5.59786, 3) (94.17, 107.12)	(4.32507, 1) (131.51, 165.41)	(4.25006, 1) (116.25, 132.59)	(4.20691, 1) (108.26, 115.68)	(4.18341, 1) (104.19, 107.34)	(4.15833, 1) (100.09, 99.18)
0.8	(5.24848, 2) (68.84, 98.57)	(5.15810, 2) (59.51, 76.51)	(5.10598, 2) (54.99, 66.70)	(5.07755, 2) (52.77, 62.15)	(5.04713, 2) (50.56, 57.86)	(4.32507, 1) (73.77, 93.95)	(4.25006, 1) (64.51, 72.67)	(4.20691, 1) (60.00, 63.15)	(4.18341, 1) (57.77, 58.73)	(4.15833, 1) (55.57, 54.55)
1.0	(5.24848, 2) (38.22, 54.46)	(5.15810, 2) (33.32, 42.88)	(5.10598, 2) (30.99, 38.00)	(5.07755, 2) (29.85, 35.77)	(5.04713, 2) (28.72, 33.65)	(4.32507, 1) (42.46, 52.02)	(4.25006, 1) (37.50, 40.75)	(4.20691, 1) (35.13, 35.98)	(4.18341, 1) (33.97, 33.79)	(4.15833, 1) (32.81, 31.73)
1.5	(5.24848, 2) (11.50, 15.41)	(5.15810, 2) (10.42, 13.21)	(5.10598, 2) (9.89, 12.22)	(5.07755, 2) (9.63, 11.75)	(5.04713, 2) (9.36, 11.29)	(4.32507, 1) (14.17, 14.75)	(4.25006, 1) (13.02, 12.59)	(4.20691, 1) (12.45, 11.63)	(4.18341, 1) (12.17, 11.17)	(4.15833, 1) (11.88, 10.72)
2.0	(4.38281, 1) (4.97, 5.99)	(4.30700, 1) (4.63, 5.39)	(4.26335, 1) (4.46, 5.10)	(4.23957, 1) (4.37, 4.96)	(4.21416, 1) (4.28, 4.81)	(4.32507, 1) (6.85, 6.06)	(4.25006, 1) (6.47, 5.45)	(4.20691, 1) (6.27, 5.16)	(4.18341, 1) (6.17, 5.01)	(4.15833, 1) (6.06, 4.87)
$n = 5$										
0.2	(4.31365, 15) (267.63, 366.84)	(4.28885, 16) (246.40, 325.43)	(4.28578, 17) (231.56, 296.10)	(4.29723, 18) (222.56, 278.02)	(4.30403, 19) (212.18, 256.48)	(3.61710, 5) (272.75, 322.02)	(3.65677, 6) (253.27, 284.28)	(3.62302, 6) (239.75, 257.61)	(3.68290, 7) (231.57, 240.94)	(3.66129, 7) (222.14, 221.30)
0.4	(4.12888, 11) (114.88, 192.02)	(4.06815, 11) (93.35, 140.10)	(4.03105, 11) (82.25, 113.30)	(4.00994, 11) (76.71, 100.49)	(3.98646, 11) (71.22, 88.46)	(3.50162, 4) (123.94, 174.88)	(3.44883, 4) (103.28, 127.91)	(3.41684, 4) (92.50, 103.37)	(3.39878, 4) (87.08, 91.52)	(3.37882, 4) (81.67, 80.27)
0.6	(3.94347, 8) (40.22, 72.93)	(3.80982, 7) (31.97, 48.44)	(3.77493, 7) (28.31, 39.10)	(3.75511, 7) (26.59, 35.11)	(3.73310, 7) (24.92, 31.53)	(3.35471, 3) (47.35, 69.20)	(3.30393, 3) (38.91, 46.37)	(3.27317, 3) (35.08, 37.38)	(3.25583, 3) (33.26, 33.51)	(3.23673, 3) (31.48, 30.01)
0.8	(3.67795, 5) (15.26, 25.85)	(3.62323, 5) (12.68, 18.24)	(3.58993, 5) (11.53, 15.44)	(3.57104, 5) (10.98, 14.23)	(3.55010, 5) (10.45, 13.11)	(3.15165, 2) (19.82, 25.80)	(3.10355, 2) (16.98, 18.27)	(3.07456, 2) (15.69, 15.46)	(3.05826, 2) (15.06, 14.24)	(3.04026, 2) (14.45, 13.11)
1.0	(3.55529, 4) (6.97, 10.49)	(3.50219, 4) (6.09, 8.09)	(3.46991, 4) (5.68, 7.14)	(3.30076, 3) (5.47, 6.71)	(3.28137, 3) (5.27, 6.31)	(3.15165, 2) (9.96, 10.86)	(3.10355, 2) (8.92, 8.42)	(3.07456, 2) (8.42, 7.45)	(3.05826, 2) (8.18, 7.01)	(3.04026, 2) (7.93, 6.59)
1.5	(3.18790, 2) (2.06, 2.14)	(3.13960, 2) (1.94, 1.87)	(3.11039, 2) (1.88, 1.74)	(3.09390, 2) (1.85, 1.68)	(3.07570, 2) (1.82, 1.62)	(2.81571, 1) (3.52, 2.48)	(2.77213, 1) (3.37, 2.19)	(2.74595, 1) (3.28, 2.06)	(2.73124, 1) (3.24, 1.99)	(2.71512, 1) (3.20, 1.93)
2.0	(3.18790, 2) (1.24, 0.69)	(3.13960, 2) (1.21, 0.63)	(3.11039, 2) (1.20, 0.59)	(3.09390, 2) (1.19, 0.58)	(3.07570, 2) (1.18, 0.56)	(2.81571, 1) (2.30, 0.91)	(2.77213, 1) (2.26, 0.84)	(2.74595, 1) (2.24, 0.81)	(2.73124, 1) (2.23, 0.79)	(2.71512, 1) (2.22, 0.77)

Table 3

K, L, ARL_1 and $SDRL_1$ values of the optimal synthetic t chart when $n \in \{7, 9\}$, $m \in \{10, 20, 40, 80, +\infty\}$, $\tau^* = 1.0$ and $ARL_0 = 370.40$ for both zero- and steady-state cases.

	Zero State					Steady State				
	$m = 10$	$m = 20$	$m = 40$	$m = 80$	$m = +\infty$	$m = 10$	$m = 20$	$m = 40$	$m = 80$	$m = +\infty$
δ^*	(K, L) $(ARL_1, SDRL_1)$	(K, L) $(ARL_1, SDRL_1)$	(K, L) $(ARL_1, SDRL_1)$	(K, L) $(ARL_1, SDRL_1)$	(K, L) $(ARL_1, SDRL_1)$	(K, L) $(ARL_1, SDRL_1)$	(K, L) $(ARL_1, SDRL_1)$	(K, L) $(ARL_1, SDRL_1)$	(K, L) $(ARL_1, SDRL_1)$	(K, L) $(ARL_1, SDRL_1)$
$n = 7$										
0.2	(3.70829, 23)	(3.67525, 24)	(3.65972, 25)	(3.65655, 26)	(3.63547, 26)	(3.28133, 9)	(3.23573, 9)	(3.20729, 9)	(3.22817, 10)	(3.20943, 10)
	(221.92, 339.64)	(193.02, 281.02)	(173.88, 240.26)	(162.80, 216.08)	(150.64, 188.96)	(230.03, 294.85)	(203.73, 243.86)	(186.32, 208.46)	(176.23, 187.25)	(165.10, 163.78)
0.4	(3.51146, 14)	(3.46388, 14)	(3.40531, 13)	(3.38807, 13)	(3.33788, 12)	(3.13411, 6)	(3.02480, 5)	(2.99800, 5)	(2.98262, 5)	(2.96529, 5)
	(63.79, 124.54)	(48.33, 79.35)	(41.35, 60.16)	(38.10, 52.11)	(34.99, 44.90)	(73.48, 115.22)	(58.12, 74.66)	(50.99, 57.00)	(47.61, 49.38)	(44.34, 42.61)
0.6	(3.29198, 8)	(3.19547, 7)	(3.16759, 7)	(3.15145, 7)	(3.13320, 7)	(2.88258, 3)	(2.84157, 3)	(2.81618, 3)	(2.80165, 3)	(2.78529, 3)
	(16.72, 31.77)	(13.29, 20.19)	(11.84, 16.29)	(11.16, 14.67)	(10.51, 13.23)	(22.19, 31.97)	(18.36, 20.68)	(16.69, 16.74)	(15.90, 15.10)	(15.13, 13.62)
0.8	(3.11006, 5)	(2.98226, 4)	(2.95597, 4)	(2.94081, 4)	(2.92373, 4)	(2.73592, 2)	(2.69649, 2)	(2.67226, 2)	(2.65840, 2)	(2.64284, 2)
	(5.89, 9.17)	(5.08, 6.75)	(4.71, 5.84)	(4.53, 5.43)	(4.36, 5.05)	(8.89, 10.01)	(7.87, 7.42)	(7.41, 6.44)	(7.18, 6.01)	(6.95, 5.60)
1.0	(2.91503, 3)	(2.87394, 3)	(2.84846, 3)	(2.83380, 3)	(2.81731, 3)	(2.73592, 2)	(2.69649, 2)	(2.67226, 2)	(2.65840, 2)	(2.64284, 2)
	(2.86, 3.56)	(2.61, 2.88)	(2.49, 2.60)	(2.43, 2.47)	(2.37, 2.34)	(4.75, 4.04)	(4.42, 3.31)	(4.25, 3.00)	(4.17, 2.86)	(4.09, 2.72)
1.5	(2.76222, 2)	(2.72277, 2)	(2.69841, 2)	(2.68444, 2)	(2.66879, 2)	(2.73592, 2)	(2.69649, 2)	(2.67226, 2)	(2.65840, 2)	(2.64284, 2)
	(1.23, 0.68)	(1.20, 0.61)	(1.19, 0.57)	(1.18, 0.55)	(1.17, 0.53)	(2.31, 0.88)	(2.27, 0.80)	(2.25, 0.76)	(2.24, 0.74)	(2.23, 0.72)
2.0	(2.76222, 2)	(2.46814, 1)	(2.44567, 1)	(2.43288, 1)	(2.41864, 1)	(5.00374, $+\infty$)	(4.92894, $+\infty$)	(4.88598, $+\infty$)	(4.85999, $+\infty$)	(4.74197, $+\infty$)
	(1.02, 0.17)	(1.02, 0.21)	(1.02, 0.19)	(1.02, 0.19)	(1.02, 0.18)	(1.63, 1.05)	(1.58, 0.97)	(1.56, 0.94)	(1.53, 0.91)	(1.53, 0.90)
$n = 9$										
0.2	(3.41643, 27)	(3.38437, 28)	(3.35642, 28)	(3.35083, 29)	(3.32082, 28)	(3.07827, 11)	(3.03738, 11)	(3.01156, 11)	(2.99648, 11)	(2.97921, 11)
	(184.85, 307.70)	(152.77, 238.65)	(132.97, 192.99)	(122.14, 167.85)	(110.82, 141.64)	(194.90, 267.40)	(165.61, 208.35)	(147.42, 169.50)	(137.39, 147.68)	(126.78, 125.06)
0.4	(3.20657, 14)	(3.14156, 13)	(3.09003, 12)	(3.07467, 12)	(3.02986, 11)	(2.89657, 6)	(2.80288, 5)	(2.77871, 5)	(2.76461, 5)	(2.74868, 5)
	(38.24, 80.79)	(28.31, 47.35)	(24.17, 35.31)	(22.29, 30.53)	(20.52, 26.39)	(46.87, 76.78)	(36.58, 46.46)	(32.11, 34.98)	(30.03, 30.31)	(28.05, 26.25)
0.6	(2.98432, 7)	(2.89594, 6)	(2.87130, 6)	(2.85689, 6)	(2.84044, 6)	(2.68539, 3)	(2.64846, 3)	(2.62533, 3)	(2.61196, 3)	(2.59683, 3)
	(8.82, 15.79)	(7.23, 10.37)	(6.56, 8.55)	(6.24, 7.79)	(5.94, 7.10)	(12.82, 16.79)	(10.92, 11.24)	(10.09, 9.33)	(9.69, 8.53)	(9.29, 7.79)
0.8	(2.80491, 4)	(2.76717, 4)	(2.74339, 4)	(2.72954, 4)	(2.62398, 3)	(2.56051, 2)	(2.52480, 2)	(2.50259, 2)	(2.48971, 2)	(2.47531, 2)
	(3.27, 4.34)	(2.93, 3.35)	(2.78, 2.96)	(2.70, 2.78)	(2.62, 2.70)	(5.39, 5.06)	(4.94, 3.97)	(4.72, 3.53)	(4.62, 3.34)	(4.51, 3.15)
1.0	(2.71276, 3)	(2.67586, 3)	(2.65270, 3)	(2.51206, 2)	(2.49750, 2)	(2.56051, 2)	(2.52480, 2)	(2.50259, 2)	(2.48971, 2)	(2.47531, 2)
	(1.80, 1.68)	(1.70, 1.41)	(1.65, 1.29)	(1.63, 1.34)	(1.60, 1.28)	(3.21, 2.07)	(3.06, 1.77)	(2.99, 1.63)	(2.95, 1.57)	(2.92, 1.51)
1.5	(2.58296, 2)	(2.54726, 2)	(2.52496, 2)	(2.51206, 2)	(2.49750, 2)	(2.56051, 2)	(2.52480, 2)	(2.50259, 2)	(2.48971, 2)	(2.47531, 2)
	(1.06, 0.29)	(1.05, 0.26)	(1.05, 0.24)	(1.04, 0.23)	(1.04, 0.23)	(2.03, 0.47)	(2.02, 0.43)	(2.01, 0.42)	(2.01, 0.41)	(2.00, 0.40)
2.0	(2.36114, 1)	(2.32749, 1)	(2.30669, 1)	(2.29475, 1)	(2.28138, 1)	(4.42059, $+\infty$)	(4.35955, $+\infty$)	(4.31932, $+\infty$)	(4.29715, $+\infty$)	(4.27664, $+\infty$)
	(1.00, 0.07)	(1.00, 0.06)	(1.00, 0.05)	(1.00, 0.05)	(1.00, 0.05)	(1.15, 0.43)	(1.13, 0.40)	(1.12, 0.37)	(1.12, 0.36)	(1.11, 0.36)

Table 4

K, L and $EARL_1$ values of the optimal synthetic t chart when $n \in \{3, 5, 7, 9\}$, $m \in \{10, 20, 40, 80, +\infty\}$, $\tau^* = 1.0$, $EARL_0 = 370.40$ and $\delta \sim U[0.1, 2.0]$, for the zero- and steady-state cases.

	$m = 10$	$m = 20$	$m = 40$	$m = 80$	$m = +\infty$
n	(K, L, $EARL_1$)	(K, L, $EARL_1$)	(K, L, $EARL_1$)	(K, L, $EARL_1$)	(K, L, $EARL_1$)
			Zero State		
3	(5.24848, 2, 87.59)	(5.15810, 2, 81.10)	(5.10598, 2, 77.50)	(5.07755, 2, 75.58)	(5.04713, 2, 73.57)
5	(3.86705, 7, 48.68)	(3.80982, 7, 43.06)	(3.77493, 7, 39.89)	(3.75511, 7, 38.17)	(3.80706, 8, 36.34)
7	(3.37914, 10, 34.49)	(3.37000, 11, 29.61)	(3.34082, 11, 26.86)	(3.32388, 11, 25.37)	(3.33788, 12, 23.78)
9	(3.18283, 13, 26.85)	(3.14156, 13, 22.56)	(3.13863, 14, 20.15)	(3.12306, 14, 18.86)	(3.10516, 14, 17.49)
			Steady State		
3	(4.32510, 1, 90.89)	(4.25007, 1, 84.52)	(4.20692, 1, 80.99)	(4.18344, 1, 79.11)	(4.15835, 1, 77.14)
5	(3.35469, 3, 52.31)	(3.30390, 3, 46.85)	(3.27319, 3, 43.78)	(3.25585, 3, 42.12)	(3.23670, 3, 40.35)
7	(2.98690, 4, 37.81)	(2.94469, 4, 33.11)	(2.99802, 5, 30.45)	(2.98262, 5, 29.02)	(2.96528, 5, 27.49)
9	(2.89657, 6, 29.90)	(2.85755, 6, 25.76)	(2.83300, 6, 23.44)	(2.81870, 6, 22.19)	(2.80243, 6, 20.87)

Table 5

Summary statistics of the Phase-I and Phase-II data for the measurements of the epitaxial layer thickness (in micrometre, μm) across wafers in the silicon epitaxy process.

Phase-I			Phase-II				
Sample number, i	$\bar{X}_i$	S_i	Sample number, i	$\bar{Y}_i$	S_i	$\hat{T}_i$	CRL
1	13.96022	0.20009	21	14.16325	0.16452	2.14633	
2	13.95122	0.20739	22	14.04661	0.14033	0.65769	
3	13.96633	0.12525	23	14.18978	0.14808	2.78518	
4	13.96396	0.13056	24	13.99877	0.11120	– 0.13195	
5	13.98608	0.12335	25	14.03681	0.10380	0.67826	
6	13.95595	0.11937	26	13.91548	0.10249	– 1.96029	
7	14.08939	0.07712	27	14.11495	0.16800	1.45905	
8	13.94601	0.10740	28	14.13336	0.11694	2.44819	
9	13.98752	0.10858	29	14.10324	0.05265	4.15788	9
10	13.94035	0.11045	30	14.04236	0.22020	0.37601	
11	14.00667	0.10712	31	14.16798	0.07874	**4.61916**	**2**
12	14.04393	0.09168	32	14.08217	0.21063	0.81571	
13	13.93254	0.10568	33	14.29147	0.12598	**5.07903**	**2**
14	14.02252	0.10442	34	14.15669	0.08378	**4.03997**	**1**
15	14.11183	0.14103	35	13.99742	0.14609	– 0.12113	
16	14.11137	0.14946	36	13.90390	0.15816	– 1.43406	
17	13.99017	0.15963	37	13.91939	0.17123	– 1.12231	
18	14.05479	0.18674	38	14.04660	0.04602	2.00511	
19	14.03861	0.19757	39	13.94265	0.08371	– 1.67424	
20	14.04719	0.21306	40	13.90240	0.14373	– 1.60128	

Remark: The boldfaced values represent the out-of-control cases.

Highlights

- The synthetic *t* chart with estimated process mean is proposed.
- Both the zero- and steady-state cases are considered.
- The run-length properties of the synthetic *t* chart are derived when μ_0 is estimated.
- Two design strategies are developed for deterministic and unknown shift sizes.
- Comparative studies show the robustness of the proposed chart over other charts.